

A New Analytical Approximation of the Fluid Antenna System Channel

Malek Khammassi, Abla Kammoun, *Member, IEEE*,
and Mohamed-Slim Alouini, *Fellow, IEEE*

Abstract

Fluid antenna systems (FAS) are an emerging technology that promises a significant diversity gain even in the smallest spaces. Motivated by the groundbreaking potentials of liquid antennas, researchers in the wireless communication community are investigating a novel antenna system where a single antenna can freely switch positions along a small linear space to pick the strongest received signal. However, the FAS positions do not necessarily follow the ever-existing rule separating them by at least half the radiation wavelength. Previous work in the literature parameterized the channels of the FAS ports simply enough to provide a single-integral expression of the probability of outage and various insights on the achievable performance. Nevertheless, this channel model may not accurately capture the correlation between the ports, given by Jake's model. This work builds on the state-of-the-art and accurately approximates the FAS channel while maintaining analytical tractability. The approximation is performed in two stages. The first stage approximation considerably reduces the number of multi-fold integrals in the probability of outage expression, while the second stage approximation provides a single integral representation of the FAS probability of outage. Further, the performance of such innovative technology is investigated under a less-idealized correlation model. Numerical results validate our approximations of the FAS channel model and demonstrate a limited performance gain under realistic assumptions. Further, our work opens the door for future research to investigate scenarios in which the FAS provides a performance gain compared to the current multiple antennas solutions.

Index Terms

Diversity, fluid antennas, MIMO, multiple antennas, selection combining, outage probability, correlated channels.

I. INTRODUCTION

For the past few decades, multiple-input multiple-output (MIMO) has been one of the most celebrated wireless communication technologies. The philosophy behind MIMO consists of

exploiting multi-path, which for so long has been considered undesirable, to multiply the capacity. Although the earliest ideas relating capacity gain to multi-path were hard to accept, MIMO has shown an undeniable performance gain, and therefore, it has become an essential component of wireless communication standards. MIMO allows data multiplexing over channels undergoing independent fading. However, the rule of thumb is to keep the antennas spatially separated by at least half the radiation wavelength to ensure a diversity gain.

The authors in [1]–[4] have recently questioned this rule. Motivated by the recent trend of using liquid metals such as Galinstan and ionized solutions such as sodium chloride for antennas [5]–[10], Wong *et al.* hypothesize a system where a single antenna can switch locations instantly in a small linear space and refer to it as a fluid antenna system (FAS). They refer to the possible positions of the antenna as ports, and they investigate a scenario where the antenna can switch to the port with the strongest received signal in the manner of traditional selection combining. This system can ensure the implementation of multiple antennas at the receiver's side without space limitations. In [1], the analysis of the first-order statistics of FAS shows a probability of outage that decreases, without a floor, as the number of ports increases. Furthermore, it shows that for a large enough number of ports, FAS can outperform maximal-ratio combining (MRC). In [2], the second-order statistics have been studied, where Wong *et al.* derived the ergodic capacity and lower-bounded it. They also derived the level crossing rate and the average fade duration of FAS. Their analysis shows a considerable capacity gain resulting from the diversity hidden in the small space of FAS. In [3], an extension of FAS for multiple access has been proposed. The analysis of the outage probability and average outage capacity characterizes the multiplexing gain of the fluid antenna multiple access, and shows its capability to support hundreds of users using only one fluid antenna at each user. Further, the problem of port selection was addressed in [4]. In fact, selecting the port with the strongest signal might necessitate the processing of a large number of observations from all the ports, which may be unfeasible in practice. Instead, the authors in [4] propose to observe a few ports and use a combination of machine learning methods and analytical approximation to show that only 10% of the ports provide more than an order of magnitude reduction in the outage probability.

The state-of-the-art works demonstrate considerable potential for the arising technology of FAS. Nevertheless, assessing its achievable performance depends entirely on diversity reception over highly correlated channels that follow Jake's model [11]. Although, closed-form or single folded integrals have been derived for the probability of outage over independent channels [12],

they are usually challenging to obtain for diversity receptions over arbitrarily correlated channels. More specifically, the probability of outage of an N-branch selection combiner in a multi-antenna system is written in terms of the multivariate cumulative distribution function (CDF) of the channel gains. However, for correlated fading channels, these CDFs have intractable expressions involving nested integrals of the Marcum Q-function. An extensive attention has been dedicated, in the literature, to derive tractable mathematical expressions for the multivariate probability density functions (PDFs) and CDFs of these distributions. One category of approaches considers arbitrary covariance matrices, however, it restricts the number of branches. For instance, simplified CDF representations have been derived for selection combining over correlated channels for bivariate [13]–[16], trivariate and quadrivariate distributions [17]–[20]. Another category of approaches considers an arbitrary number of branches but restricts the covariance matrix to specific forms. For instance, the constant correlation model was heavily studied in the literature, and simplified CDF expressions were derived [21], [22]. A more generalized covariance model was considered in [23]–[25]. Nevertheless, the covariance matrix was constrained to a certain form as in [24, equation (2)]. Two main forms of these distributions are generally provided: (i) infinite-summation forms as in [13], [16], [17], [20], which can be truncated to give a certain approximation of the distribution. However, infinite summation CDFs may be computationally expensive. (ii) single-integral forms as in [21]–[25], which provide insights and a considerable computational gain. The most general framework to derive the distribution of an N-branch selection combiner over correlated channels provides an N multi-fold integral expression [26], which is not insightful or computationally efficient. The authors in [1] parameterize the channel coefficients as in [24], which simplifies the derivation of the probability of outage. However, although this parameterization is an essential first step towards gaining insight into the technology, it imposes a structure on the covariance model that may not accurately capture the dependence between the FAS ports given by Jake’s model.

This paper aims to study the performance of the FAS under a more accurate correlation model that closely follows Jake’s model. More specifically, we propose a tractable expression for the probability of outage that closely approximates the simulation results of FAS. The approximation is made in two stages. In the first stage, the number of multi-fold integrals in the probability of outage is considerably reduced. In the second stage, we investigate a more insightful probability of outage expression by approximating the result of the first stage approximation with a power of a single integral. Numerical results validate the approximations

and show a limited gain under realistic conditions. Therefore, careful modeling and analysis of the FAS channel is required to determine scenarios where this technology can outperform traditional multiple antennas technologies.

The remainder of this paper is organized as follows. In section II, we present the FAS channel. In section III, our proposed FAS channel model is presented. Our model provides both an exact and an approximated FAS channel representation. However, unlike the exact modeling, the approximated modeling of the FAS channel gives more tractable expression for probability of outage. Section IV presents our numerical results and section V provides some concluding remarks.

Notation: We use boldface upper and lower case letters for matrices and column vectors, respectively. $E[.]$, $V[.]$ and $Cov[.,.]$ denote the statistical expectation, variance and covariance respectively. $(.)^T$ and $|.|$ stand for the transpose and magnitude respectively and $(.)_{m,n}$ denotes the element in row m and column n . Finally, CN denotes the circularly-symmetric complex normal distribution.

II. FAS CHANNEL

In this paper, we follow the same abstraction of FAS as in [1]. We consider a single antenna that can move freely along N equally distributed positions (i.e., ports) on a linear space of length $W\lambda$, where λ is the wavelength of the radiation, as it is shown in fig. 1. Therefore, taking the first port as a reference point, the distance between the first port and the k -th port is given by

$$\Delta d_{k,1} = \frac{k-1}{N-1}W\lambda, \text{ for } k = 1, 2, \dots, N. \quad (1)$$

The received signal by the k -th port can be modeled as

$$y_k = g_k x + n_k, \text{ for } k = 1, 2, \dots, N. \quad (2)$$

where x is the transmitted data symbol, $n_k \sim CN(0, \sigma_n^2)$ is the additive white Gaussian noise (AWGN) at the k -th port, and $g_k \sim CN(0, \sigma^2)$ is the flat fading coefficient at the k -th port. Furthermore, we assume that the channel coefficients of $\mathbf{g} = (g_1, g_2, \dots, g_N)^T$ are correlated with a covariance matrix Σ_g . Assuming two dimensional isotropic scattering with an isotropic receiver port, as in [1], the spatial separation between the ports of FAS yields to a difference

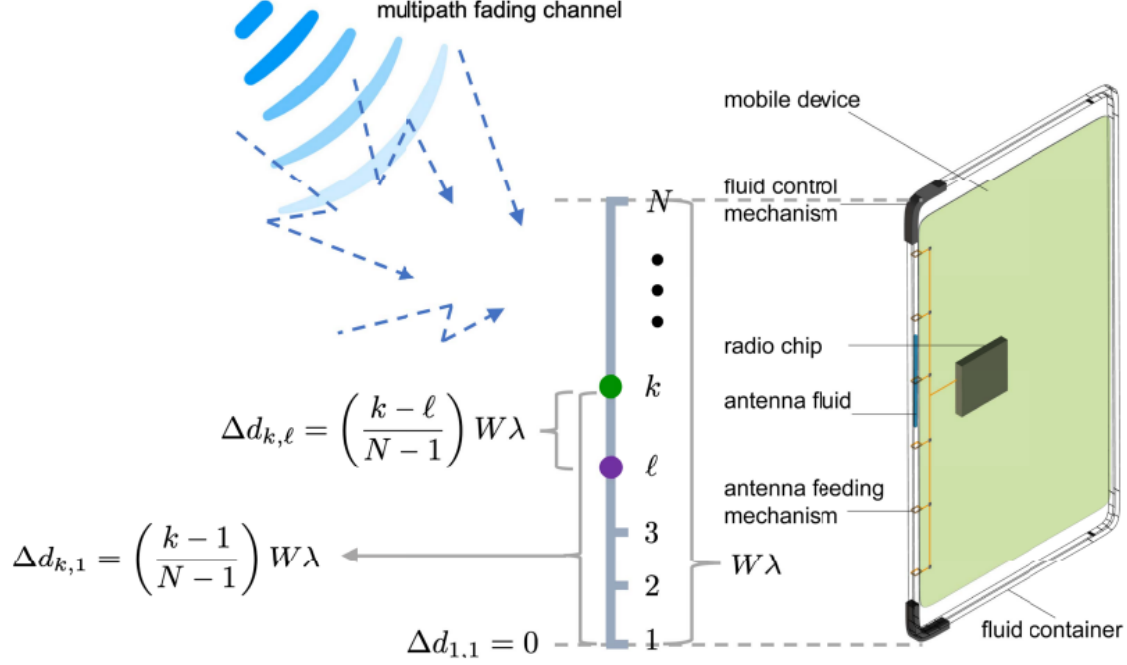


Fig. 1: Architecture of FAS [1].

in the phases of arriving paths, thus inducing correlation between the channels following Jake's model [11] as

$$(\mathbf{\Sigma}_g)_{k,\ell} = \text{Cov}[g_k, g_\ell] = \sigma^2 J_0 \left(2\pi \frac{\Delta d_{k,\ell}}{\lambda} \right) = \sigma^2 J_0 \left(\frac{2\pi(k-\ell)}{N-1} W \right). \quad (3)$$

where $J_0(\cdot)$ is the zero-order Bessel function of the first kind.

Further, the average signal-to-noise ratio (SNR) at each port is given by

$$\Gamma = \frac{\sigma^2 E[|x|]^2}{\sigma_n^2} = \sigma^2 \Theta, \quad (4)$$

where $\Theta \triangleq \frac{E[|x|]^2}{\sigma_n^2}$. Assuming that the FAS can instantly switch to the maximum gain of the channel coefficients as in [1], the channel gain of the FAS is then given by

$$g_{FAS} = \max \{|g_1|, |g_2|, \dots, |g_N|\}. \quad (5)$$

III. PROPOSED FAS CHANNEL MODEL

A. General Model for Arbitrarily Correlated Rayleigh Channels

We propose to represent a set of correlated Rayleigh fading channels h_1, h_2, \dots, h_N as

$$h_k = \sigma_h \sqrt{1 - \sum_{l=1}^M \alpha_{k,l}^2} (x_k + jy_k) + \sigma_h \sum_{l=1}^M \alpha_{k,l} (a_l + jb_l), \quad (6)$$

where $x_1, \dots, x_N, y_1, \dots, y_N, a_1, \dots, a_M, b_1, \dots, b_M$ are independent and identically distributed (i.i.d) normal random variables with zero-mean and variance $\frac{1}{2}$. Furthermore, $\alpha_{1,1}, \dots, \alpha_{1,M}, \dots, \alpha_{N,1}, \dots, \alpha_{N,M}$, M and σ_h are parameters to be chosen according to the different correlations between the channels. We can see that according to the model

$$h_k \sim \mathcal{CN}(0, \sigma_h^2) \quad \forall k \in \{1, \dots, N\}, \quad (7)$$

$$(\mathbf{\Sigma}_h)_{i,j} = \begin{cases} \sigma_h^2 & \text{if } i = j \\ \sigma_h^2 \sum_{l=1}^M \alpha_{i,l} \alpha_{j,l} & \text{if } i \neq j \end{cases}, \quad (8)$$

where $\mathbf{\Sigma}_h$ is the covariance matrix of $\mathbf{h} = (h_1, h_2, \dots, h_N)^T$ and $(\mathbf{\Sigma}_h)_{i,j}$ is its entry at (i, j) for $i, j \in \{1, \dots, N\}$.

We can see that the channel modeling in [1], [2]–[4] is a particular case of the model in (6) with $M = 1$, $\sigma_h = \sigma$, $\alpha_{1,1} = 1$ and $\alpha_{k,1} = J_0\left(\frac{2\pi(k-1)}{(N-1)}W\right)$ for $k \in \{2, \dots, N\}$. Therefore, we can see from (8) that the correlation matrix of [1] does not exactly follow Jake's model because $\text{Cov}[h_k, h_l] = \sigma^2 J_0\left(\frac{2\pi(k-1)}{(N-1)}W\right) J_0\left(\frac{2\pi(\ell-1)}{(N-1)}W\right) \neq \sigma^2 J_0\left(\frac{2\pi(k-\ell)}{(N-1)}W\right)$ for $k, \ell \in \{2, \dots, N\}$. Our channel model has more flexibility with more model parameters than the channel model considered in [1], [2]–[4]. In the following, we start by finding our model's parameters for an exact representation of $\mathbf{g} = (g_1, g_2, \dots, g_N)^T$ as in (6). Then, motivated by this representation, we choose a different set of model parameters that approximate the joint distribution of $\mathbf{g} = (g_1, g_2, \dots, g_N)^T$ while maintaining mathematical tractability of the CDF of $g_{FAS} = \max\{|g_1|, |g_2|, \dots, |g_N|\}$, under a less-idealized correlation model than the one considered in [1], [2]–[4].

B. Exact Model

In order to represent $\mathbf{g} = (g_1, g_2, \dots, g_N)^T$ as in (6), we choose the parameters σ_h , M and $\alpha_{k,l}$ for $k = 1, \dots, N$ and $l = 1, \dots, M$, such that the random vectors $\mathbf{g} = (g_1, g_2, \dots, g_N)^T$ and $\mathbf{h} = (h_1, h_2, \dots, h_N)^T$ have the same joint distribution. In other words, since a multivariate complex Gaussian distribution is fully defined by its mean vector and its covariance matrix, we

investigate the model parameters ensuring that \mathbf{g} and \mathbf{h} have the same mean vector and covariance matrix.

Theorem III.1. *If $\sigma_h = \sigma$, then $\mathbf{g} = (g_1, g_2, \dots, g_N)^T$ and $\mathbf{h} = (h_1, h_2, \dots, h_N)^T$ have the same marginal distributions, independently from the choice of M and $\alpha_{k,l}$, $k \in \{1, \dots, N\}$, $l \in \{1, \dots, M\}$.*

Proof. For $k \in \{1, \dots, N\}$,

$$E[h_k] = E[g_k] = 0, \quad (9)$$

$$V[h_k] = \sigma_h^2 \left(1 - \sum_{l=1}^M \alpha_{k,l}^2\right) + \sigma_h^2 \sum_{l=1}^M \alpha_{k,l}^2 \quad (10)$$

$$= \sigma_h^2 = \sigma^2 = V[g_k]. \quad (11)$$

Since g_k and h_k are circularly-symmetric complex normal random variables, then they have the same distribution $\forall k \in \{1, \dots, N\}$. \square

Since (9) shows that \mathbf{g} and \mathbf{h} have the same mean vector, then, in order for them to have the same joint distribution, it suffices to choose the model parameters in (6) such that $\mathbf{\Sigma}_h = \mathbf{\Sigma}_g$.

Theorem III.2. *If $\sigma_h = \sigma$, $M = N$ and $\alpha_{k,l} = \frac{\sqrt{s_l}}{\sigma} u_{k,l}$, $1 \leq k, l \leq N$, where s_1, s_2, \dots, s_N are the non-increasingly ordered eigenvalues of $\mathbf{\Sigma}_g$ and $\mathbf{u}_1, \mathbf{u}_2, \dots, \mathbf{u}_N$ are their respective associated eigenvectors with $\mathbf{u}_l = (u_{1,l}, u_{2,l}, \dots, u_{N,l})^T$ for $l \in \{1, 2, \dots, N\}$, then $\mathbf{g} = (g_1, g_2, \dots, g_N)^T$ and $\mathbf{h} = (h_1, h_2, \dots, h_N)^T$ have the same joint distribution. In this case, $\mathbf{g} = (g_1, g_2, \dots, g_N)^T$ can be represented using model (6) as*

$$g_k \stackrel{d}{=} \sum_{l=1}^N \sqrt{s_l} u_{k,l} (a_l + j b_l), \text{ for } k \in \{1, \dots, N\}, \quad (12)$$

where the operator $\stackrel{d}{=}$ denotes equality in the sense of distribution.

Proof. See Appendix A. \square

We can see that the model parameters choice in theorem III.2 provides an exact representation of the correlated channel vector \mathbf{g} using model (6). Nevertheless, the representation in (12) is only in terms of the random variables $a_1, \dots, a_N, b_1, \dots, b_N$ and does not include the random variables $x_1, \dots, x_N, y_1, \dots, y_N$. This is due to the choice of model parameters making $\sum_{l=1}^M \alpha_{k,l}^2 = 1$, and thus, multiplying the terms $\{x_k + jy_k, \forall k \in \{1, \dots, N\}\}$ by zeros in the

model (Appendix A). However, the random variables $x_1, \dots, x_N, y_1, \dots, y_N$ can be very useful in deriving the CDF of $g_{FAS} = \max \{|g_1|, |g_2|, \dots, |g_N|\}$, as it will be shown in the following. In the case of the exact model, the CDF of the selection combiner over $\mathbf{g} = (g_1, g_2, \dots, g_N)^T$, and equivalently, the CDF of the FAS channel, can only be written in the form of N-fold integrals for $N > 3$ [27]. To further simplify the expression of the CDF, we approximate the joint distribution of $\mathbf{g} = (g_1, g_2, \dots, g_N)^T$ using the same model (6) in two stages.

C. Approximated Model

1) First Stage Approximation:

Definition III.1. We define the random vector $\hat{\mathbf{g}} = (\hat{g}_1, \hat{g}_2, \dots, \hat{g}_N)^T$, the approximation of the channel vector $\mathbf{g} = (g_1, g_2, \dots, g_N)^T$, as

$$\hat{g}_k = \sqrt{\sigma^2 - \sum_{l=1}^{\epsilon\text{-rank}} s_l u_{k,l}^2} (x_k + jy_k) + \sum_{l=1}^{\epsilon\text{-rank}} \sqrt{s_l} u_{k,l} (a_l + jb_l), \quad \forall k \in \{1, \dots, N\}, \quad (13)$$

where $\epsilon\text{-rank}$ is the number of its eigenvalues of Σ_g exceeding a threshold $\epsilon > 0$, $s_1, s_2, \dots, s_{\epsilon\text{-rank}}$ are the non-increasingly ordered eigenvalues of Σ_g greater than ϵ and $\mathbf{u}_1, \mathbf{u}_2, \dots, \mathbf{u}_{\epsilon\text{-rank}}$ are their respective associated eigenvectors with $\mathbf{u}_l = (u_{1,l}, u_{2,l}, \dots, u_{N,l})^T$ for $l \in \{1, 2, \dots, \epsilon\text{-rank}\}$.

Similarly to the exact model (theorem III.2), definition III.1 of the approximation takes the parameters $\sigma_h = \sigma$ and $\alpha_{k,l} = \frac{\sqrt{s_l}}{\sigma} u_{k,l}$, $1 \leq k \leq N$, $1 \leq l \leq M$. However, unlike the exact representation where $M = N$, we introduce more flexibility to the approximation by taking $M = \epsilon\text{-rank}$ for $\epsilon > 0$. Then, we investigate the choice of $\epsilon > 0$, and equivalently the choice of $\epsilon\text{-rank}$, that provides an analytically tractable approximation of the CDF of $g_{FAS} = \max \{|g_1|, |g_2|, \dots, |g_N|\}$ while ensuring that $\hat{\mathbf{g}} = (\hat{g}_1, \hat{g}_2, \dots, \hat{g}_N)^T$ is close to $\mathbf{g} = (g_1, g_2, \dots, g_N)^T$ in the sense of distribution.

Theorem III.3. Consider the random vector $\mathbf{g} = (g_1, g_2, \dots, g_N)^T$ and its approximation $\hat{\mathbf{g}} = (\hat{g}_1, \hat{g}_2, \dots, \hat{g}_N)^T$ given in definition in III.1.

$$\hat{\mathbf{g}} \xrightarrow{d} \mathbf{g}, \text{ as } \epsilon \rightarrow 0. \quad (14)$$

Proof. See Appendix B. □

Theorem III.4. Consider the random vector $\mathbf{g} = (g_1, g_2, \dots, g_N)^T$ and its approximation $\hat{\mathbf{g}} = (\hat{g}_1, \hat{g}_2, \dots, \hat{g}_N)^T$ given in definition in III.1.

$$\max \{|\hat{g}_1|, |\hat{g}_2|, \dots, |\hat{g}_N|\} \xrightarrow{d} \max \{|g_1|, |g_2|, \dots, |g_N|\} = g_{FAS}, \text{ as } \epsilon \rightarrow 0. \quad (15)$$

Proof. We define $f : \mathbb{C}^N \rightarrow \mathbb{R}$ as $f(z_1, \dots, z_N) = \max\{|z_1|, \dots, |z_N|\}$. The function f is continuous, and we have $\hat{\mathbf{g}} \xrightarrow{d} \mathbf{g}$, as $\epsilon \rightarrow 0$. Therefore, by the continuous mapping theorem [28], $f(\hat{\mathbf{g}}) \xrightarrow{d} f(\mathbf{g})$, as $\epsilon \rightarrow 0$. \square

By combining theorems III.3 and III.4, we can approximate $g_{FAS} = \max\{|g_1|, \dots, |g_N|\}$ by approximating the channel vector $\mathbf{g} = (g_1, \dots, g_N)^T$. Furthermore, the approximation improves (in the sense of distribution) as ϵ decreases, which in turn increases ϵ -rank. Therefore, the best possible approximation is obtained by maximizing ϵ -rank and taking it equal to N . However, if $M = \epsilon\text{-rank} = N$ then, by theorem III.2, we obtain an exact representation of the channel vector $\mathbf{g} = (g_1, \dots, g_N)^T$ in terms of only the random variables a_1, \dots, a_N and b_1, \dots, b_N . In this case, the CDF of the FAS channel can only be written in the form of N -fold integrals for $N > 3$ [27].

On the other hand, including the random variables $x_1, \dots, x_N, y_1, \dots, y_N$ in the representation of the approximation can lead to a more simplified expression of the joint CDF of $(|g_1|, \dots, |g_N|)$, and consequently, the CDF of $g_{FAS} = \max\{|g_1|, |g_2|, \dots, |g_N|\}$. In fact, by representing \mathbf{g} in terms of $x_1, \dots, x_N, y_1, \dots, y_N$, the random vector $(|g_1|, \dots, |g_N|)$ becomes independent conditionally on $a_1, \dots, a_M, b_1, \dots, b_M$. As a result, the conditional joint CDF of the channel magnitudes becomes the product of the conditional CDFs of each channel magnitude, which constitutes the first step into deriving the CDF of the FAS channel. Hence, we choose ϵ such that the approximation in definition III.1 remains in terms of all the random variables $x_1, \dots, x_N, y_1, \dots, y_N, a_1, \dots, a_M$ and b_1, \dots, b_M . In other words, we choose $\epsilon\text{-rank} < N$ so that $\sum_{l=1}^{\epsilon\text{-rank}} s_l u_{k,l}^2 < \sigma^2$, guaranteeing that $x_1, \dots, x_N, y_1, \dots, y_N$ are multiplied by non-zero scalar in the approximation. Then, we derive the expressions of the approximated CDF and probability of outage of the FAS channel in what follows.

Theorem III.5 (Joint Cumulative Distribution Function).

Consider the approximation $\hat{\mathbf{g}} = (\hat{g}_1, \hat{g}_2, \dots, \hat{g}_N)^T$ given in definition in III.1 for $\epsilon > 0$ such that

$\epsilon\text{-rank} < N$. The joint CDF of $|\hat{g}_1|, |\hat{g}_2|, \dots, |\hat{g}_N|$ is given by

$$\begin{aligned}
& F_{|\hat{g}_1|, |\hat{g}_2|, \dots, |\hat{g}_N|}(r_1, r_2, \dots, r_N) \\
&= \int \cdots \int \prod_{l=1}^{\epsilon\text{-rank}} \frac{1}{\pi} \exp(-(a_l^2 + b_l^2)) \\
& \quad \prod_{k=1}^N \left(1 - Q_1 \left(\frac{\sqrt{2 \left(\sum_{l=1}^{\epsilon\text{-rank}} \sqrt{s_l} u_{k,l} a_l \right)^2 + 2 \left(\sum_{l=1}^{\epsilon\text{-rank}} \sqrt{s_l} u_{k,l} b_l \right)^2}}{\sqrt{\sigma^2 - \sum_{l=1}^{\epsilon\text{-rank}} s_l u_{k,l}^2}}, \frac{\sqrt{2} r_k}{\sqrt{\sigma^2 - \sum_{l=1}^{\epsilon\text{-rank}} s_l u_{k,l}^2}} \right) \right) \\
& \quad da_1 \dots da_{\epsilon\text{-rank}} db_1 \dots db_{\epsilon\text{-rank}}.
\end{aligned} \tag{16}$$

Proof. See Appendix C. \square

Theorem III.6 (Cumulative Distribution Function).

Consider the approximation $\hat{\mathbf{g}} = (\hat{g}_1, \hat{g}_2, \dots, \hat{g}_N)^T$ given in definition in III.1 for $\epsilon > 0$ such that $\epsilon\text{-rank} < N$. The CDF of $\max\{|\hat{g}_1|, \dots, |\hat{g}_N|\}$ is given by

$$\begin{aligned}
& F_{\max\{|\hat{g}_1|, \dots, |\hat{g}_N|\}}(r) \\
&= \int \cdots \int \prod_{l=1}^{\epsilon\text{-rank}} \frac{1}{\pi} \exp(-(a_l^2 + b_l^2)) \\
& \quad \prod_{k=1}^N \left(1 - Q_1 \left(\frac{\sqrt{2 \left(\sum_{l=1}^{\epsilon\text{-rank}} \sqrt{s_l} u_{k,l} a_l \right)^2 + 2 \left(\sum_{l=1}^{\epsilon\text{-rank}} \sqrt{s_l} u_{k,l} b_l \right)^2}}{\sqrt{\sigma^2 - \sum_{l=1}^{\epsilon\text{-rank}} s_l u_{k,l}^2}}, \frac{\sqrt{2} r}{\sqrt{\sigma^2 - \sum_{l=1}^{\epsilon\text{-rank}} s_l u_{k,l}^2}} \right) \right) \\
& \quad da_1 \dots da_{\epsilon\text{-rank}} db_1 \dots db_{\epsilon\text{-rank}}.
\end{aligned} \tag{17}$$

Proof.

$$\begin{aligned}
F_{\max\{|\hat{g}_1|, \dots, |\hat{g}_N|\}}(r) &= P(|\hat{g}_1| < r, \dots, |\hat{g}_N| < r) \\
&= F_{|\hat{g}_1|, \dots, |\hat{g}_N|}(r, \dots, r)
\end{aligned} \tag{18}$$

\square

To approximate the outage probability of the FAS channel, we define the outage event as

$$\{g_{\text{FAS}}^2 \Theta < \gamma_{\text{th}}\} = \left\{ g_{\text{FAS}} < \sqrt{\frac{\gamma_{\text{th}}}{\Theta}} \right\} = \left\{ \max\{|g_1|, \dots, |g_N|\} < \sqrt{\frac{\gamma_{\text{th}}}{\Theta}} \right\}. \tag{19}$$

Therefore, the probability of outage can be approximated by

$$P_{out}(\gamma_{th}) \approx P \left\{ \max\{|\hat{g}_1|, \dots, |\hat{g}_N|\} < \sqrt{\frac{\gamma_{th}}{\Theta}} \right\}. \quad (20)$$

Theorem III.7 (Outage Probability).

Consider the approximation $\hat{\mathbf{g}} = (\hat{g}_1, \hat{g}_2, \dots, \hat{g}_N)^T$ given in definition in III.1 for $\epsilon > 0$ such that $\epsilon\text{-rank} < N$. We approximate the outage probability of the FAS channel as

$$P_{out}(\gamma_{th}) \approx \int \cdots \int \prod_{l=1}^{\epsilon\text{-rank}} \frac{1}{\pi} \exp(-(a_l^2 + b_l^2)) \prod_{k=1}^N \left(1 - Q_1 \left(\frac{\sqrt{2 \left(\sum_{l=1}^{\epsilon\text{-rank}} \sqrt{s_l} u_{k,l} a_l \right)^2 + 2 \left(\sum_{l=1}^{\epsilon\text{-rank}} \sqrt{s_l} u_{k,l} b_l \right)^2}}{\sqrt{\sigma^2 - \sum_{l=1}^{\epsilon\text{-rank}} s_l u_{k,l}^2}}, \frac{\sqrt{2} \sqrt{\frac{\gamma_{th}}{\Theta}}}{\sqrt{\sigma^2 - \sum_{l=1}^{\epsilon\text{-rank}} s_l u_{k,l}^2}} \right) \right) da_1 \dots da_{\epsilon\text{-rank}} db_1 \dots db_{\epsilon\text{-rank}}. \quad (21)$$

Proof.

$$P_{out}(\gamma_{th}) \approx P \left\{ \max\{|\hat{g}_1|, |\hat{g}_2|, \dots, |\hat{g}_N|\} < \sqrt{\frac{\gamma_{th}}{\Theta}} \right\} \quad (22)$$

$$= F_{|\hat{g}_1|, |\hat{g}_2|, \dots, |\hat{g}_N|} \left(\sqrt{\frac{\gamma_{th}}{\Theta}}, \sqrt{\frac{\gamma_{th}}{\Theta}}, \dots, \sqrt{\frac{\gamma_{th}}{\Theta}} \right). \quad (23)$$

Therefore, the expression follows directly from replacing r by $\sqrt{\frac{\gamma_{th}}{\Theta}}$ in (17). \square

Theorems III.6 and III.7 present approximated expressions for the CDF and probability of outage of the FAS channel that depend on the parameter ϵ . In what follows, we investigate the impact of this parameter on both the accuracy and the mathematical tractability of these approximated expressions.

Proposition 1. Let $\epsilon > 0$ be big enough that $\epsilon\text{-rank} < \frac{N}{2}$. Then, the number of the multi-fold integrals in the approximated CDF and outage probability of the FAS channel is reduced by $\frac{N-2}{N} \epsilon\text{-rank}$.

Proof. We can see from theorems III.6 and III.7 that we need $2 \times \epsilon\text{-rank}$ multi-fold integrals to approximate the CDF and outage probability of the FAS channel. Originally, the CDF of the selection combiner over correlated channels is represented by N multi-fold integrals [29].

Therefore, the number of multi-fold integrals is reduced by $\frac{N-2}{N} \frac{\epsilon\text{-rank}}{N}$ using this approximation. \square

Proposition 1 shows a reduction in the number of multi-fold integrals as ϵ increases (i.e. ϵ -rank decreases), while theorem III.4 shows a higher accuracy of the approximation as ϵ decreases (i.e. ϵ -rank increases). Therefore, we have to undergo the trade-off between tractability and accuracy. In practice (as the numerical results illustrate in section IV), we can find an ϵ big enough to have a considerable reduction in the number of multi-fold integrals while guaranteeing a high accuracy of the approximation. However, we can see that finding a suitable ϵ is not enough to evaluate the expressions of the approximations. The approximated probability of outage and CDF do not depend explicitly on ϵ , but instead on ϵ -rank. Therefore, we need to count the number of eigenvalues of Σ_g exceeding ϵ , which numerically is a straightforward task. However, determining ϵ -rank as a function of the problem parameters (i.e. N and W) is more insightful and provides stand-alone expressions of the FAS channel distribution and probability of outage. In what follows, we investigate the eigenvalue distribution function of the covariance matrix Σ_g to approximate the number of its eigenvalues exceeding a certain threshold.

Theorem III.8. *Consider the matrix \mathbf{T}_N of size $N \times N$ such that*

$$(\mathbf{T}_N)_{(k,\ell)} = J_0(2\pi(k-\ell)c), \text{ for } k, \ell \in \{1, \dots, N\} \text{ and } 0 < c < \frac{1}{2}.$$

Let $\{s_{N,k}; k = 1, \dots, N\}$ be the set of its eigenvalues. Consider the eigenvalue distribution function of \mathbf{T}_N defined as $D_N(x) = (\text{number of } s_{N,k} \leq x) / N$, and its limiting distribution $D(x) = \lim_{N \rightarrow \infty} D_N(x)$.

$$D(x) = \begin{cases} 1 - 2c & \text{if } 0 < x < \frac{\sigma^2}{\pi c} \\ 1 - 2c + \sqrt{(2c)^2 - \frac{4\sigma^4}{(\pi x)^2}} & \text{if } x \geq \frac{\sigma^2}{\pi c}, \end{cases} \quad (24)$$

Proof. See Appendix D. \square

We can see from theorem III.8 that for a small enough threshold x , the fraction of eigenvalues of \mathbf{T}_N less than x (as N goes to infinity) become independent of x , and always equal to $1 - 2c$. This result allows us to approximate the ϵ -rank of the covariance matrix Σ_g . In fact, we can see that for $c = \frac{W}{N-1}$, $\Sigma_g = \mathbf{T}_N$. Therefore, for a small $0 < \epsilon < \frac{\sigma^2}{\pi c}$ and a large N , the fraction

of eigenvalues of Σ_g less than ϵ can be approximated by $1 - \frac{2W}{N-1}$. Therefore, the fraction of eigenvalues exceeding ϵ can be approximated by $\frac{2W}{N-1}$. Thus,

$$\epsilon\text{-rank} \approx 2W \frac{N}{N-1}, \text{ for large } N \text{ and } 0 < \epsilon < \frac{\sigma^2(N-1)}{\pi W}. \quad (25)$$

The approximation above is more accurate as N goes to infinity. We observe through simulation that the asymptotic convergence is slow, and the approximation of ϵ -rank becomes accurate for very large N beyond the range we test for FAS. Therefore, we propose to approximate ϵ -rank as follows

$$\epsilon\text{-rank} \approx a W \frac{N}{N-1}, \text{ for large } N \text{ and } 0 < \epsilon < \frac{\sigma^2(N-1)}{\pi W}. \quad (26)$$

where a is a constant that we determine in the numerical results section to approximate ϵ -rank better for the tested range of N .

Even though the practical values of ϵ -rank are quite small compared to $\frac{N}{2}$, multi-fold integral representation of the CDF and probability of outage still restricts us from gaining insights about the FAS. Therefore, we design a second stage approximation of the channel vector to further simplify the CDF expression.

2) Second Stage Approximation:

In the first stage approximation, we use the random vector $\hat{\mathbf{g}} = (\hat{g}_1, \dots, \hat{g}_N)^T$ to approximate the distribution of the channel vector $\mathbf{g} = (g_1, \dots, g_N)^T$. Then, we approximate the FAS channel distribution $g_{FAS} = \max\{|g_1|, \dots, |g_N|\}$ by the distribution of $\max\{|\hat{g}_1|, \dots, |\hat{g}_N|\}$. The second stage approximation aims to further approximate the distribution of $\max\{|\hat{g}_1|, \dots, |\hat{g}_N|\}$. However, it starts by approximating the joint distribution of a set of independent copies of $\hat{\mathbf{g}} = (\hat{g}_1, \hat{g}_2, \dots, \hat{g}_N)^T$, then uses it to retrieve an approximation of the CDF of $\max\{|\hat{g}_1|, \dots, |\hat{g}_N|\}$.

Definition III.2. Let $\mathbf{z} = (z_1, \dots, z_N)^T$ be a random vector. A set of R copies of \mathbf{z} is defined as the set of random vectors $\{\mathbf{z}^{(r)} = (z_{1,r}, \dots, z_{N,r})^T, 1 \leq r \leq R\}$ such that, $\forall r \in \{1, \dots, R\}$, \mathbf{z} and $\mathbf{z}^{(r)}$ have the same joint distribution.

The copies of \mathbf{z} are said to be independent if $\forall r, q \in \{1, \dots, R\}$ such that $r \neq q$, $\mathbf{z}^{(r)}$ and $\mathbf{z}^{(q)}$ are independent. In other words,

$$\forall r, q \in \{1, \dots, R\}, \forall k, l \in \{1, \dots, N\}, \text{Cov}(z_{k,q}, z_{l,r}) = \text{Cov}(z_{k,q}, z_{l,r})\delta(r - q). \quad (27)$$

The copies of \mathbf{z} are said to be dependent if $\exists r, q \in \{1, \dots, R\}$ such that $r \neq q$, and $\mathbf{z}^{(r)}$ and $\mathbf{z}^{(q)}$ are dependent. In other words,

$$\exists r, q \in \{1, \dots, R\} \text{ with } r \neq q \text{ and } \exists k, l \in \{1, \dots, N\} \text{ such that } \text{Cov}(z_{k,q}, z_{l,r}) \neq 0. \quad (28)$$

In this second stage approximation, we relate the joint distribution of independent copies of the correlated random vector $\hat{\mathbf{g}} = (\hat{g}_1, \hat{g}_2, \dots, \hat{g}_N)^T$ to the joint distribution of correlated copies of some independent random vector $\tilde{\mathbf{g}} = (\tilde{g}_1, \tilde{g}_2, \dots, \tilde{g}_N)^T$ that we design. In other words, if we consider two random matrices $\hat{\mathbf{G}}$ and $\tilde{\mathbf{G}}$, where the columns of $\hat{\mathbf{G}}$ are the copies of $\hat{\mathbf{g}}$, and the columns of $\tilde{\mathbf{G}}$ are the copies of $\tilde{\mathbf{g}}$, then $\hat{\mathbf{G}}$ has independent columns and dependent rows, while $\tilde{\mathbf{G}}$ has dependent columns and independent rows. In the following, we start by formally defining the matrices $\hat{\mathbf{G}}$ and $\tilde{\mathbf{G}}$. Then, we investigate their distributions (*i.e.* mean vectors and covariance matrices). Next, we tune the distribution of $\tilde{\mathbf{G}}$ to approximate the distribution of $\hat{\mathbf{G}}$. Finally, by exploiting how $\hat{\mathbf{G}}$ and $\hat{\mathbf{g}}$ are related, we obtain the CDF of $\max\{|\hat{g}_1|, \dots, |\hat{g}_N|\}$ from the CDF of a function of the elements of $\hat{\mathbf{G}}$ which, in turn, is approximated by the CDF of a function of the elements of $\tilde{\mathbf{G}}$. This allows us to retrieve an approximation of the distribution of $\max\{|\hat{g}_1|, \dots, |\hat{g}_N|\}$ from the distribution of $\tilde{\mathbf{G}}$ that we carefully design to avoid a multi-fold integral representation of the approximated CDF.

Definition III.3. Let $\epsilon > 0$ such that $\epsilon\text{-rank} < N$. We define the random matrix $\hat{\mathbf{G}}$ of size $N \times R$ such that its (k, r) entry is written as

$$\hat{g}_{k,r} = \sqrt{\sigma^2 - \sum_{l=1}^{\epsilon\text{-rank}} s_l u_{k,l}^2} (x_{k,r} + jy_{k,r}) + \sum_{l=1}^{\epsilon\text{-rank}} \sqrt{s_l} u_{k,l} (a_{l,r} + jb_{l,r}), \quad 1 \leq k \leq N, \quad 1 \leq r \leq R, \quad (29)$$

where $\{x_{k,r}, y_{k,r}, a_{l,r}, b_{l,r}, 1 \leq r \leq R, 1 \leq k \leq N, 1 \leq l \leq \epsilon\text{-rank}\}$ is a set of i.i.d normal random variables with zero-mean and variance $\frac{1}{2}$.

Corollary III.8.1. Consider the random matrix $\hat{\mathbf{G}}$ for $\epsilon > 0$ such that $\epsilon\text{-rank} < N$.

- 1) The columns of $\hat{\mathbf{G}}$ are copies of $\hat{\mathbf{g}} = (\hat{g}_1, \dots, \hat{g}_N)^T$.
- 2) The columns of $\hat{\mathbf{G}}$ are independent.
- 3) The rows of $\hat{\mathbf{G}}$ are dependent.

Proof. See Appendix E. □

Proposition 2. Consider the random matrix $\hat{\mathbf{G}}$ for $\epsilon > 0$ such that $\epsilon\text{-rank} < N$. If we arrange the elements of matrix $\hat{\mathbf{G}}$ as $(\hat{g}_{1,1}, \dots, \hat{g}_{N,1}, \dots, \hat{g}_{1,R}, \dots, \hat{g}_{N,R})^T$, then its mean vector $\boldsymbol{\mu}_{\hat{\mathbf{G}}}$ and covariance matrix $\boldsymbol{\Sigma}_{\hat{\mathbf{G}}}$ can be written as

$$\boldsymbol{\mu}_{\hat{\mathbf{G}}} = (0, 0, \dots, 0)^T. \quad (30)$$

$$\boldsymbol{\Sigma}_{\hat{\mathbf{G}}} = \begin{pmatrix} \boldsymbol{\Sigma}_{\hat{\mathbf{g}}} & 0 & \cdots & 0 \\ 0 & \boldsymbol{\Sigma}_{\hat{\mathbf{g}}} & \cdots & 0 \\ \vdots & \vdots & \ddots & \vdots \\ 0 & 0 & \cdots & \boldsymbol{\Sigma}_{\hat{\mathbf{g}}} \end{pmatrix} \quad (31)$$

where $\boldsymbol{\Sigma}_{\hat{\mathbf{g}}}$ is the covariance matrix of $\hat{\mathbf{g}}$, and its entry at (i, j) is written as

$$(\boldsymbol{\Sigma}_{\hat{\mathbf{g}}})_{i,j} = \begin{cases} \sigma^2 & \text{if } i = j \\ \sum_{l=1}^{\epsilon\text{rank}} s_l u_{i,l} u_{j,l} & \text{if } i \neq j, \end{cases} \quad \text{for } i, j \in \{1, \dots, N\}. \quad (32)$$

Proof. See Appendix F. □

Now that $\hat{\mathbf{G}}$ is defined and its distribution is determined (*i.e.* mean vector and covariance matrix), we investigate its relationship with the distribution of $\max\{|\hat{g}_1|, \dots, |\hat{g}_N|\}$ in the next theorem.

Theorem III.9. Consider the random matrix $\hat{\mathbf{G}}$ for $\epsilon > 0$ such that $\epsilon\text{-rank} < N$. Let Ω_R be the maximum magnitude of the elements of $\hat{\mathbf{G}}$ defined as

$$\Omega_R = \max\{|\hat{g}_{k,r}|, \ 1 \leq k \leq N, \ 1 \leq r \leq R\}. \quad (33)$$

Then, the CDF of Ω_R is given by

$$F_{\Omega_R}(g) = (F_{\max\{|\hat{g}_1|, \dots, |\hat{g}_N|\}}(g))^R. \quad (34)$$

Proof.

$$\begin{aligned} F_{\Omega_R}(g) &= P(|\hat{g}_k^{(r)}| \leq g, \ \forall k \in \{1, \dots, N\}, \ \forall r \in \{1, \dots, R\}) \\ &= \left(P(|\hat{g}_k^{(r)}| \leq g, \ \forall 1 \leq k \leq N) \right)^R \\ &= (F_{\max\{|\hat{g}_1|, |\hat{g}_2|, \dots, |\hat{g}_N|\}}(g))^R \end{aligned} \quad (35)$$

because the columns of $\hat{\mathbf{G}}$ are independent copies of $\hat{\mathbf{g}} = (\hat{g}_1, \dots, \hat{g}_N)^T$. □

We can see from theorem III.9 that the CDF of $\max\{|\hat{g}_1|, |\hat{g}_2|, \dots, |\hat{g}_N|\}$ is a power of the CDF of a function of the elements of $\hat{\mathbf{G}}$. In the following, we approximate the joint distribution of $\hat{\mathbf{G}}$ by the joint distribution of a random matrix $\tilde{\mathbf{G}}$ that we design. This allows us to approximate the distribution of a function of the elements of $\hat{\mathbf{G}}$ by the distribution of the same function of the elements of $\tilde{\mathbf{G}}$. This eventually leads to a simpler approximation of the distribution of $\max\{|\hat{g}_1|, |\hat{g}_2|, \dots, |\hat{g}_N|\}$.

Definition III.4. Let $\epsilon > 0$ such that $\epsilon\text{-rank} < N$. We define the random matrix $\tilde{\mathbf{G}}$ of size $N \times R$ such that its (k, r) entry is written as

$$\tilde{g}_{k,r} = \sqrt{\sigma^2 - \sum_{l=1}^{\epsilon\text{-rank}} s_l u_{k,l}^2} (x_{k,r} + j y_{k,r}) + \sum_{l=1}^{\epsilon\text{-rank}} \sqrt{s_l} u_{k,l} (a_{l,k} + j b_{l,k}), \quad 1 \leq k \leq N, \quad 1 \leq r \leq R, \quad (36)$$

where $\{x_{k,r}, y_{k,r}, a_{l,k}, b_{l,k}, 1 \leq r \leq R, 1 \leq k \leq N, 1 \leq l \leq \epsilon\text{-rank}\}$ is a set of i.i.d normal random variables with zero-mean and variance $\frac{1}{2}$.

Corollary III.9.1. Consider the random matrix $\tilde{\mathbf{G}}$ for $\epsilon > 0$ such that $\epsilon\text{-rank} < N$.

- 1) The columns of $\tilde{\mathbf{G}}$ are copies of $\tilde{\mathbf{g}} = (\tilde{g}_1, \dots, \tilde{g}_N)^T$.
- 2) The columns of $\tilde{\mathbf{G}}$ are dependent.
- 3) The rows of $\tilde{\mathbf{G}}$ are independent.

where $\tilde{\mathbf{g}}$ is defined such that

$$\tilde{g}_k = \sqrt{\sigma^2 - \sum_{l=1}^{\epsilon\text{-rank}} s_l u_{k,l}^2} (x_k + j y_k) + \sum_{l=1}^{\epsilon\text{-rank}} \sqrt{s_l} u_{k,l} (a_{l,k} + j b_{l,k}), \quad 1 \leq k \leq N. \quad (37)$$

Proof. See Appendix G. □

Proposition 3. Consider the random matrix $\tilde{\mathbf{G}}$ for $\epsilon > 0$ such that $\epsilon\text{-rank} < N$. If we arrange the elements of matrix $\tilde{\mathbf{G}}$ as $(\tilde{g}_{1,1}, \dots, \tilde{g}_{1,R}, \dots, \tilde{g}_{N,1}, \dots, \tilde{g}_{N,R})^T$, then its mean vector $\boldsymbol{\mu}_{\tilde{\mathbf{G}}}$ and covariance matrix $\boldsymbol{\Sigma}_{\tilde{\mathbf{G}}}$ can be written as

$$\boldsymbol{\mu}_{\tilde{\mathbf{G}}} = (0, 0, \dots, 0)^T. \quad (38)$$

$$\boldsymbol{\Sigma}_{\tilde{\mathbf{G}}} = \begin{pmatrix} \boldsymbol{\Sigma}_1 & 0 & \cdots & 0 \\ 0 & \boldsymbol{\Sigma}_2 & \cdots & 0 \\ \vdots & \vdots & \ddots & \vdots \\ 0 & 0 & \cdots & \boldsymbol{\Sigma}_N \end{pmatrix} \quad (39)$$

where $\mathbf{\Sigma}_k$, $k \in \{1, \dots, N\}$, is the $R \times R$ matrix such that its entry at (i, j) is written as

$$(\mathbf{\Sigma}_k)_{i,j} = \begin{cases} \sigma^2 & \text{if } i = j \\ \sum_{l=1}^{\epsilon\text{-rank}} s_l u_{k,l}^2 & \text{if } i \neq j \end{cases} \text{ for } i, j \in \{1, \dots, R\}. \quad (40)$$

Proof. See Appendix H. \square

Theorem III.10. Consider the random matrix $\tilde{\mathbf{G}}$ for $\epsilon > 0$ such that $\epsilon\text{-rank} < N$. Let Ψ_R be the maximum magnitude of the elements of $\tilde{\mathbf{G}}$ defined as

$$\Psi_R = \max\{|\tilde{g}_{k,r}|, 1 \leq k \leq N, 1 \leq r \leq R\}. \quad (41)$$

Then, the CDF of Ψ_R can be written as

$$F_{\Psi_R}(g) = \prod_{k=1}^N \int_0^{+\infty} \frac{1}{\sum_{l=1}^{\epsilon\text{-rank}} s_l u_{k,l}^2} \exp\left(-\frac{r}{\sum_{l=1}^{\epsilon\text{-rank}} s_l u_{k,l}^2}\right) \left(1 - Q_1\left(\frac{\sqrt{2}r}{\sqrt{\sigma^2 - \sum_{l=1}^{\epsilon\text{-rank}} s_l u_{k,l}^2}}, \frac{\sqrt{2}g}{\sqrt{\sigma^2 - \sum_{l=1}^{\epsilon\text{-rank}} s_l u_{k,l}^2}}\right)\right)^R dr. \quad (42)$$

Proof. See Appendix I. \square

We design the random matrix $\tilde{\mathbf{G}}$ such that $F_{\max\{|\tilde{g}_{k,r}|, 1 \leq k \leq N, 1 \leq r \leq R\}}$ is a product of single integrals, as it is shown in theorem III.10. Now, if we choose R such that the distribution of $\tilde{\mathbf{G}}$ approximates the distribution of $\hat{\mathbf{G}}$ in a certain sense, then the distribution of $\max\{|\tilde{g}_{k,r}|, 1 \leq k \leq N, 1 \leq r \leq R\}$ will also approximate the distribution of $\max\{|\hat{g}_{k,r}|, 1 \leq k \leq N, 1 \leq r \leq R\}$, resulting in a single-integral approximation of the CDF of $\max\{|\hat{g}_{k,r}|, 1 \leq k \leq N, 1 \leq r \leq R\}$. On the other hand, theorem III.9 shows that $F_{\max\{|\hat{g}_1|, \dots, |\hat{g}_N|\}} = F_{\max\{|\hat{g}_{k,r}|, 1 \leq k \leq N, 1 \leq r \leq R\}}^{\frac{1}{R}}$. Therefore, the latter approximation allows us to write CDF of $\max\{|\hat{g}_1|, \dots, |\hat{g}_N|\}$ as a power of single integrals instead of the initial multi-fold integrals. In the following, we investigate the choice of R that allows to approximate $\hat{\mathbf{G}}$ by $\tilde{\mathbf{G}}$ in the sense of a distance that we define.

Definition III.5. Let CN_0 denote the family of multivariate circularly-symmetric complex normal distributions with zero-mean. We define a distance between two distributions F and G in CN_0 with respective covariance matrices Σ_F and Σ_G as

$$d(F, G) = \|\Sigma_F - \Sigma_G\|_1, \quad (43)$$

where $\|\cdot\|_1$ is the induced matrix norm 1 (i.e. the maximum absolute column sum of the matrix).

In the following, we denote the covariance matrices of $\hat{\mathbf{G}}$ and $\tilde{\mathbf{G}}$ given in propositions 2 and 3, respectively, by $\Sigma_{\hat{\mathbf{G}}}(R)$ and $\Sigma_{\tilde{\mathbf{G}}}(R)$ to emphasize their dependence on R , and we use the well-defined distance measure above to approximate $\hat{\mathbf{G}}$ by $\tilde{\mathbf{G}}$.

Definition III.6. Let $\epsilon > 0$ such that ϵ -rank $< N$. Consider the random matrices $\hat{\mathbf{G}}$ and $\tilde{\mathbf{G}}$ with covariance matrices $\Sigma_{\hat{\mathbf{G}}}(R)$ and $\Sigma_{\tilde{\mathbf{G}}}(R)$, respectively. We define R_1^* as the solution to the following optimization problem

$$\min_{R \in \{1, \dots, N\}} \|\Sigma_{\hat{\mathbf{G}}}(R) - \Sigma_{\tilde{\mathbf{G}}}(R)\|_1 \quad (P1)$$

We can see that R_1^* minimizes the distance in (43) between $\hat{\mathbf{G}}$ and $\tilde{\mathbf{G}}$. Therefore, it makes sense to assume that the distribution of $\tilde{\mathbf{G}}$ approximates the distribution of $\hat{\mathbf{G}}$ for $R = R_1^*$. However, solving the above optimization problem is not straight forward. Therefore, we relax (P1) by (P2) defined in the following, where the feasible set $\{1, \dots, N\}$ becomes restricted to the set of divisors of N .

Definition III.7. Let $\epsilon > 0$ such that ϵ -rank $< N$. Consider the random matrices $\hat{\mathbf{G}}$ and $\tilde{\mathbf{G}}$ with covariance matrices $\Sigma_{\hat{\mathbf{G}}}(R)$ and $\Sigma_{\tilde{\mathbf{G}}}(R)$, respectively. We define R_2^* as the solution to the following relaxed optimization problem

$$\min_{R \text{ divisor of } N} \|\Sigma_{\hat{\mathbf{G}}}(R) - \Sigma_{\tilde{\mathbf{G}}}(R)\|_1 \quad (P2)$$

Relaxing the optimization problem (P1) simplifies the feasible set. Nevertheless, the objective function is still not straight forward to minimize even on the relaxed feasible set. Therefore, we simplify the objective function in an approximated optimization problem (P3) defined in the following.

Definition III.8. Consider the covariance matrix Σ_g of the channel vector $\mathbf{g} = (g_1, \dots, g_N)^T$. We define R_3^* as the solution to the following optimization problem

$$\min_{R \text{ divisor } N} \|\Sigma_G(R) - \sigma^2 \mathbb{I}(R)\|_1 \quad (P3)$$

where $\Sigma_G(R)$ and $\mathbb{I}(R)$ are the $NR \times NR$ matrices defined as

$$\Sigma_G(R) = \begin{pmatrix} \Sigma_g & 0 & \cdots & 0 \\ 0 & \Sigma_g & \cdots & 0 \\ \vdots & \vdots & \ddots & \vdots \\ 0 & 0 & \cdots & \Sigma_g \end{pmatrix} \quad \mathbb{I}(R) = \begin{pmatrix} \mathbf{1}_{R \times R} & 0 & \cdots & 0 \\ 0 & \mathbf{1}_{R \times R} & \cdots & 0 \\ \vdots & \vdots & \ddots & \vdots \\ 0 & 0 & \cdots & \mathbf{1}_{R \times R} \end{pmatrix} \quad (44)$$

with $\mathbf{1}_{R \times R}$ is the $R \times R$ constant matrix with all entries equal to 1.

Next, we investigate the accuracy of approximating the objective function in (P1) by the objective function in (P3) in the following theorem.

Theorem III.11. *Let $\epsilon > 0$ such that ϵ -rank $< N$. Consider the random matrices $\hat{\mathbf{G}}$ and $\tilde{\mathbf{G}}$ with covariance matrices $\Sigma_{\hat{\mathbf{G}}}(R)$ and $\Sigma_{\tilde{\mathbf{G}}}(R)$, respectively. For $\epsilon = \frac{\epsilon'}{2N}$, $\epsilon' > 0$, we have*

$$\left| \left\| \Sigma_{\hat{\mathbf{G}}}(R) - \Sigma_{\tilde{\mathbf{G}}}(R) \right\|_1 - \left\| \Sigma_G(R) - \sigma^2 \mathbb{I}(R) \right\|_1 \right| < \epsilon'. \quad (45)$$

Proof. See Appendix J. □

We can see that taking $\epsilon = \frac{\epsilon'}{2N}$ for a small enough $\epsilon' > 0$ ensures that the objective functions in (P2) and (P3) are very comparable. This justifies approximating the solution of (P2) by the solution of (P3).

Theorem III.12. *The solution to the optimization problem (P3) is given by R_3^* , the greatest divisor of N , verifying*

$$J_0 \left(\frac{2\pi(R_3^* - 1)}{N - 1} W \right) \leq 0.5. \quad (46)$$

Proof. See Appendix K. □

Theorem III.12 shows that the optimal solution of (P3) is the greatest divisor of N verifying equation (46). Since, $J_0(1.52) \approx 0.5$, R_3^* is the greatest divisor of N verifying

$$R_3^* \leq \left\lfloor \frac{1.52(N - 1)}{2\pi W} \right\rfloor. \quad (47)$$

We propose to approximate $\hat{\mathbf{G}}$ by $\tilde{\mathbf{G}}$ in the sense of the distance in (43) for $R = R^* = \min \left\{ \left\lfloor \frac{1.52(N - 1)}{2\pi W} \right\rfloor, N \right\}$. This allows us to approximate the distribution of $\max\{|\hat{g}_{k,r}|, 1 \leq k \leq N, 1 \leq r \leq R^*\}$ by the distribution of $\max\{|\tilde{g}_{k,r}|, 1 \leq k \leq N, 1 \leq r \leq R^*\}$. Although, R^* is a solution of (P3) only when $\left\lfloor \frac{1.52(N - 1)}{2\pi W} \right\rfloor$ is a divisor of N , simulation results show that it accurately

approximates the distribution of $\max\{|\hat{g}_{k,r}|, 1 \leq k \leq N, 1 \leq r \leq R^*\}$ by the distribution of $\max\{|\tilde{g}_{k,r}|, 1 \leq k \leq N, 1 \leq r \leq R^*\}$ without necessarily being a divisor of N .

Theorem III.13 (Cumulative Distribution Function).

Let $\epsilon = \frac{\epsilon'}{2N} < \frac{\sigma^2(N-1)}{\pi W}$ for $\epsilon' > 0$. Then, for ϵ -rank $= \lceil aW \frac{N}{N-1} \rceil$ and $R = \min \left\{ \left\lfloor \frac{1.52(N-1)}{2\pi W} \right\rfloor, N \right\}$, the CDF of $\max\{|\hat{g}_1|, |\hat{g}_2|, \dots, |\hat{g}_N|\}$ can be approximated as

$$F_{\max\{|\hat{g}_1|, |\hat{g}_2|, \dots, |\hat{g}_N|\}}(g) \approx$$

$$\prod_{k=1}^N \left[\int_0^{+\infty} \frac{1}{\sum_{l=1}^{\epsilon\text{-rank}} s_l u_{k,l}^2} \exp\left(-\frac{r}{\sum_{l=1}^{\epsilon\text{-rank}} s_l u_{k,l}^2}\right) \left(1 - Q_1\left(\frac{\sqrt{2}r}{\sqrt{\sigma^2 - \sum_{l=1}^{\epsilon\text{-rank}} s_l u_{k,l}^2}}, \frac{\sqrt{2}g}{\sqrt{\sigma^2 - \sum_{l=1}^{\epsilon\text{-rank}} s_l u_{k,l}^2}}\right)\right)^R dr \right]^{\frac{1}{R}}. \quad (48)$$

Proof. We have $\epsilon < \frac{\sigma^2(N-1)}{\pi W}$, then, according to (26), ϵ -rank can be approximated as $aW \frac{N}{N-1}$. Further, we have $\epsilon = \frac{\epsilon'}{2N}$ for $\epsilon' > 0$, then, $F_{\Omega_R}(g) \approx F_{\Psi_R}(g)$ for $R = \min \left\{ \left\lfloor \frac{1.52(N-1)}{2\pi W} \right\rfloor, N \right\}$. On the other hand, theorem III.9 shows that

$$F_{\Omega_R}(g) = (F_{\max\{|\hat{g}_1|, |\hat{g}_2|, \dots, |\hat{g}_N|\}}(g))^R. \quad (49)$$

Therefore, $F_{\max\{|\hat{g}_1|, |\hat{g}_2|, \dots, |\hat{g}_N|\}}(g) = (F_{\Omega_R}(g))^{\frac{1}{R}} \approx (F_{\Psi_R}(g))^{\frac{1}{R}}$, and the expression in (48) is obtained by plugging in the expression of F_{Ψ_R} given in theorem III.10. \square

By approximating the CDF of $\max\{|\hat{g}_1|, |\hat{g}_2|, \dots, |\hat{g}_N|\}$, which in turn approximates the CDF of $g_{FAS} = \max\{|g_1|, \dots, |g_N|\}$. We obtain an approximation for the CDF and the probability of outage of the FAS channel.

Theorem III.14 (Outage Probability).

Let $\epsilon = \frac{\epsilon'}{2N} < \frac{\sigma^2(N-1)}{\pi W}$ for $\epsilon' > 0$. Then, for ϵ -rank $= aW \frac{N}{N-1}$ and $R = \min \left\{ \left\lfloor \frac{1.52(N-1)}{2\pi W} \right\rfloor, N \right\}$, the

probability of the outage event of the FAS channel can be approximated as

$$P_{out}(\gamma_{th}) \approx$$

$$\prod_{k=1}^N \left[\int_0^{+\infty} \frac{1}{\sum_{l=1}^{\epsilon\text{-rank}} s_l u_{k,l}^2} \exp\left(-\frac{r}{\sum_{l=1}^{\epsilon\text{-rank}} s_l u_{k,l}^2}\right) \left(1 - Q_1\left(\frac{\sqrt{2}r}{\sqrt{\sigma^2 - \sum_{l=1}^{\epsilon\text{-rank}} s_l u_{k,l}^2}}, \frac{\sqrt{2}\sqrt{\frac{\gamma_{th}}{\Theta}}}{\sqrt{\sigma^2 - \sum_{l=1}^{\epsilon\text{-rank}} s_l u_{k,l}^2}}\right)\right)^R dr \right]^{\frac{1}{R}}. \quad (50)$$

Proof.

$$\begin{aligned} p_{out}(\gamma_{th}) &= P\left\{|g_{FAS}| < \sqrt{\frac{\gamma_{th}}{\Theta}}\right\} \\ &\approx F_{\max\{|\hat{g}_1|, |\hat{g}_2|, \dots, |\hat{g}_N|\}}\left(\sqrt{\frac{\gamma_{th}}{\Theta}}\right). \end{aligned} \quad (51)$$

□

The second stage approximation allows us to further simplify the probability of outage and the CDF of the FAS. In fact, instead of N multi-fold integrals, we represent the probability of outage and the CDF as a powers of single integrals.

IV. NUMERICAL RESULTS

In this section, we start by assessing the accuracy of the first and second stage approximations. Then, we analyze the FAS performance.

In the first stage approximation, the channel vector $(g_1, \dots, g_N)^T$ is approximated by $(\hat{g}_1, \dots, \hat{g}_N)^T$ in the sense of distribution. Then, by the continuous mapping theorem, the distribution of $\max\{|g_1|, \dots, |g_N|\}$ is approximated by the distribution of $\max\{|\hat{g}_1|, \dots, |\hat{g}_N|\}$. The main intuition behind the way we design the approximation comes from the decaying profile of the eigenvalues of the covariance matrix $\mathbf{\Sigma}_g$ of the channel vector $(g_1, \dots, g_N)^T$. In fact, the covariance matrix $\mathbf{\Sigma}_g$ differs from the covariance matrix of its approximation, $\mathbf{\Sigma}_{\hat{g}}$, only at the off-diagonal elements. More precisely, we can write the (i, j) -th off-diagonal entry of $\mathbf{\Sigma}_g$ as $\sum_{l=1}^N s_l u_{i,l} u_{j,l}$, while the (i, j) -th off-diagonal entry of $\mathbf{\Sigma}_{\hat{g}}$ is written as $\sum_{l=1}^{\epsilon\text{-rank}} s_l u_{i,l} u_{j,l}$. We can see that the more decaying are the eigenvalues s_i for $i > \epsilon\text{-rank}$, the more negligible is their contribution to the sum $\sum_{l=1}^N s_l u_{i,l} u_{j,l}$. Consequently, $\sum_{l=1}^{\epsilon\text{-rank}} s_l u_{i,l} u_{j,l} \approx \sum_{l=1}^N s_l u_{i,l} u_{j,l}$ and $\mathbf{\Sigma}_{\hat{g}} \approx \mathbf{\Sigma}_g$, which improves the accuracy of the first stage approximation. In fig. 2, we plot $\frac{(\text{number of } s_k > x)}{N}$ vs x , for $\sigma = 1$, and for multiple values of N and W to illustrate the decaying

profile of the eigenvalues. For instance, for $N = 200$ and $W = 0.2$, $P(s_k > 3 \times 10^{-15})$ is less than 0.045, which means that more than 95% of the eigenvalues of Σ_g are less than 3×10^{-15} . In this case, it makes sense to take ϵ -rank = $\lfloor N \times 0.045 \rfloor = 9$ to ensure that $\hat{\mathbf{g}}$ well-approximates \mathbf{g} , and consequently, $\max\{|\hat{g}_1|, \dots, |\hat{g}_N|\}$ well-approximates $\max\{|g_1|, \dots, |g_N|\}$ in the sense of distribution. In other words, the first stage approximation considers only the contribution of the dominant eigenvalues of the covariance matrix, which well captures the correlations between the ports. Fig. 2 also demonstrates that the percentage of dominant eigenvalues decreases as N increases, and increases as W increases. For example, for a fixed $W = 2$, the eigenvalues exceeding 7.5×10^{-15} decreased from 30% to 8% when N increased from 50 to 200. On the other hand, they increased from 6.5% to 8% when W increased from 1 to 2 for a fixed $N = 200$. We recall that the length of the antenna array is $W\lambda$ and the spacing between every two ports is $\frac{W\lambda}{N-1}$. Therefore, if we fix N , the larger is W , the more decorrelated and spaced are the FAS ports. In this case, the number of dominant eigenvalues keeps increasing as we increase W to reach N when the covariance matrix becomes diagonal with diagonal elements (i.e. eigenvalues) equal to σ^2 . Furthermore, if we fix W , the larger is N , the closer and more correlated are the FAS ports and the smaller is the number of dominant eigenvalues of the covariance matrix. To conclude, fig. 2 shows that a considerable percentage of the eigenvalues of the covariance matrix can be considered negligible. Therefore, taking ϵ -rank as the number of dominant eigenvalues makes ϵ -rank $\ll N$ and ensures a considerable reduction in the number of multi-fold integrals according to proposition 1.

a) First Stage Approximation: fig. 3 shows simulations of the FAS channel versus the first stage approximation model for $W = 1$, $N = 100$ and $\sigma^2 = 10$. We compare their empirical CDFs to investigate the influence of ϵ on the accuracy of the first stage approximation. We can see that the approximation improves as ϵ decreases (i.e. as ϵ -rank increases), which confirms the result of theorem III.4. Furthermore, we can see that high accuracy is obtained by only taking ϵ -rank = $5 \ll N$. Therefore, according to proposition 1, the number of the multi-fold integrals in the approximated probability of outage is reduced by 0.9 (from 100 integrals to 10 integrals), which is a considerable computational gain.

The parameter in question, as far as the first approximation is concerned, is ϵ -rank. It can be determined numerically by counting the number of eigenvalues of Σ_g that exceed a certain

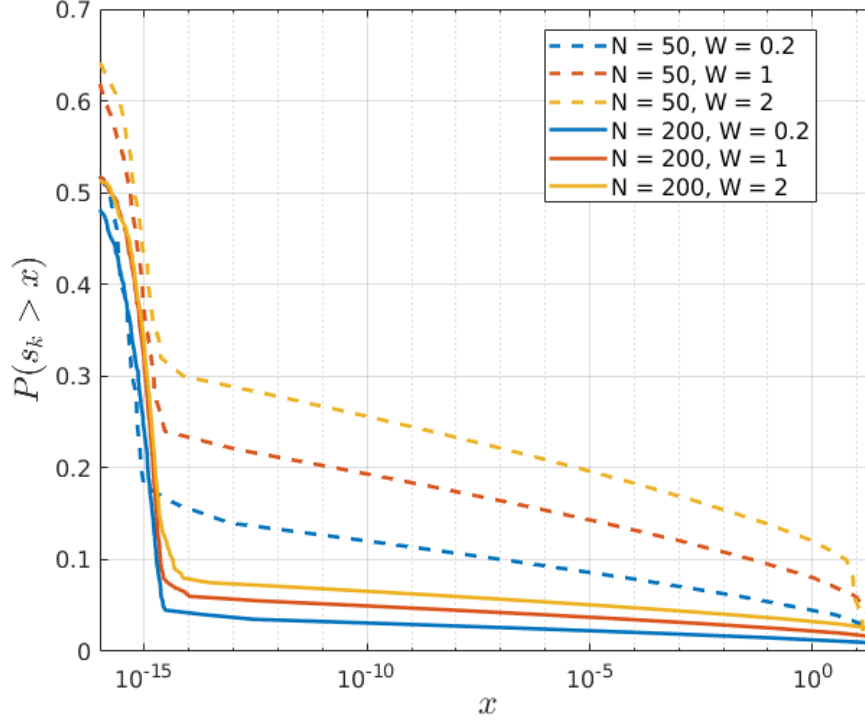


Fig. 2: Empirical complementary CDF of the eigenvalues of Σ_g for $\sigma = 1$ and different values of N and W .

threshold ϵ for given N and W . However, for more insight, we investigate how ϵ -rank varies as a function of the problem parameters N and W . First, we determine an asymptotic expression of ϵ -rank for a large N , given by theorem III.8. Then, we choose a threshold $\epsilon = \frac{\sigma^2}{2N}$. In other words, ϵ -rank will be the number of eigenvalues of Σ_g exceeding $\frac{\sigma^2}{2N}$, and the eigenvalues less than $\frac{\sigma^2}{2N}$ will be considered negligible in the first stage approximation. Now for this choice of threshold, we have on one hand that $\frac{N-1}{\pi W} > \frac{2}{\pi} \geq 0.63$ since $\frac{W}{N-1} < \frac{1}{2}$. On the other hand, $\frac{1}{2N} < 0.5$. Therefore, $\epsilon = \frac{\sigma^2}{2N} < \sigma^2 \frac{N-1}{\pi W}$, and according to theorem III.8, the expression of ϵ -rank becomes independent of ϵ , and can be approximated by $\lceil 2W \frac{N}{N-1} \rceil$ for a large N , as in (25). For more precision around the smaller values of N , we propose to approximate ϵ -rank as $\lceil aW \frac{N}{N-1} \rceil$ where a is a parameter that we determine numerically. We consider the $N \times N$ matrix \mathbf{T}_N defined such that $(\mathbf{T}_N)_{i,j} = J_0\left(\frac{2\pi W(i-j)}{N-1}\right)$ for $1 \leq i, j \leq N$. On one hand, we have $\mathbf{T}_N = \Sigma_g$ for $\sigma = 1$. On the otherhand, our choice of threshold $\epsilon = \frac{\sigma^2}{2N}$ ensures that ϵ -rank does not depend on σ^2 (theorem III.8). Therefore, finding ϵ -rank of Σ_g for an arbitrary σ^2 is equivalent to finding ϵ -

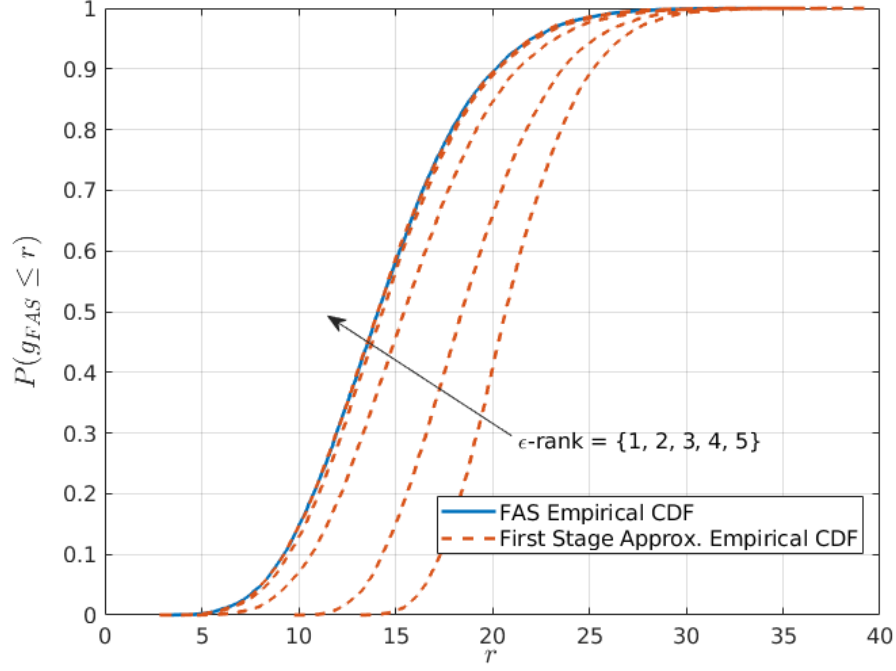


Fig. 3: Empirical CDF of FAS versus first stage approximation.

rank of \mathbf{T}_N . To determine a numerically, we simply count the number of eigenvalues exceeding $\epsilon = \frac{1}{2N}$, for $N \in \{10, \dots, 300\}$ and $W \in [0.1, 5]$. Then, we determine a that minimizes the mean squared error (MSE) between the actual ϵ -rank and the approximated ϵ -rank given by the formula ϵ -rank $= \lceil aW \frac{N}{N-1} \rceil$. The minimization of the MSE gives $a = 3.1935$. Therefore, ϵ -rank $\approx \lceil 3.1935W \frac{N}{N-1} \rceil$, which has been validated by simulation results. For instance, in fig. 3, we can see that taking ϵ -rank = 4 guarantees a satisfactory approximation of the CDF, which is also given by $\lceil 3.1935W \frac{N}{N-1} \rceil$ for $N = 100$ and $W = 1$. We also can see from the approximated expression of ϵ -rank that it varies very fast with W and slowly with N . This can also be observed in fig. 2. Further, we can see that for our target ranges of $N \in \{10, \dots, 300\}$ and $W \in [0.1, 5]$, $\lceil 3.1935W \frac{N}{N-1} \rceil \ll N$. Therefore, the values taken by ϵ -rank are very small compared to N . This again guarantees a considerable reduction in the number of multi-fold integrals of the approximation.

b) Second Stage Approximation: To further improve mathematical tractability, we design the second stage approximation that provides a single-integral expression of the CDF as in theorem III.13 and we assess its accuracy. Fig. 4 shows the empirical CDF of the FAS channel

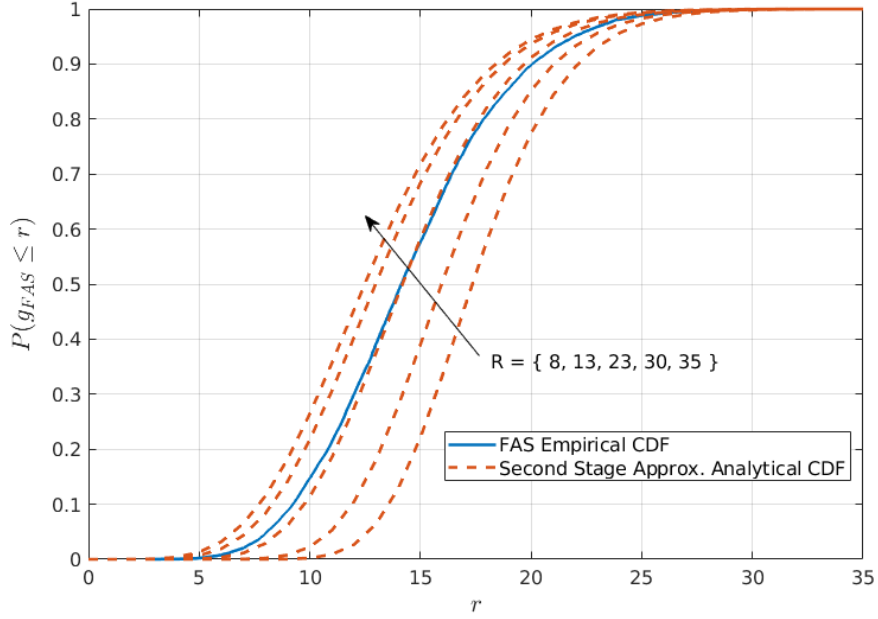


Fig. 4: Empirical CDF of FAS versus second stage approximation.

versus the analytical CDF expression given by the second stage approximation for $W = 1$, $N = 100$ and $\sigma^2 = 10$. We can see that the approximation starts improving as R increases from 8 to 13. It reaches a satisfactory approximation for $R = 23$, and as R keeps increasing from 30 to 35, the approximation starts degrading. Therefore, we investigate the optimal value of R that gives the best approximation as a function of the problem parameters. An approximated optimal value is given by $R^* = \min \left\{ \left\lfloor \frac{1.52(N-1)}{2\pi W} \right\rfloor, N \right\}$. Although the proof of optimality is provided for the relaxed problem (P3), simulation results show that R^* provides a satisfactory approximation for the general optimization problem (P1). For instance, taking the case of fig. 4, we have $R^* = \min \left\{ \left\lfloor \frac{1.52 \times 99}{2\pi} \right\rfloor, 100 \right\} = 23$.

The second stage approximation provides a satisfactory single-integral approximation of the CDF of the FAS channel. Therefore, we compare our second stage approximation CDF to the analytical CDF in [1], equation (16), and the empirical CDF of the FAS channel. In fig. 5a, we take $\sigma = 10$, we consider $N = 40$ and $N = 200$ and we fix $W = 1$. By examining the compared CDFs in fig. 5a, we can see two main observations. First, our model provides a more accurate approximation of the FAS empirical CDF. In fact, we can see that the model from [1] is optimistic because it lower-bounds the empirical CDF of the FAS channel, and therefore, it

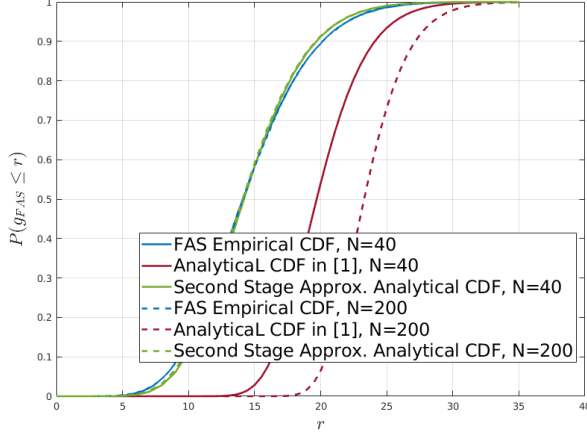
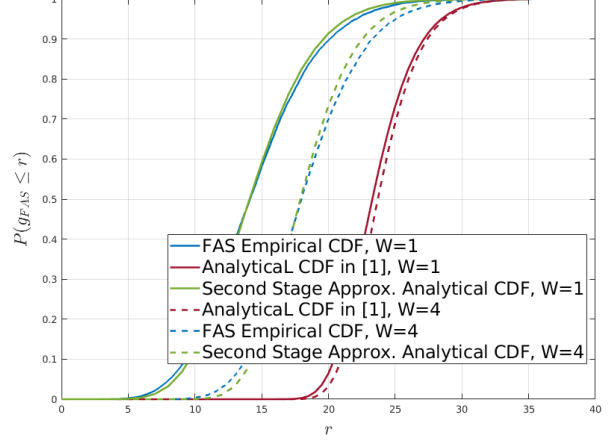
(a) Comparison for fixed $W = 1$ and $\sigma = 10$.(b) Comparison for fixed $N = 200$ and $\sigma = 10$.

Fig. 5: Empirical CDF of FAS versus analytical CDF in [1], second stage approximation CDF.

lower-bounds the probability of outage. Second, we can see that as N varies from 40 to 200, the FAS empirical CDF, as well as our approximation, remain almost unchanged. This may indicate that the probability of outage does not necessarily decrease as N increases. However, when N increases from 40 to 200, the analytical CDF in [1] significantly shifts to right indicating an optimistic decrease in the probability of outage. In fig. 5b, we take $\sigma = 10$, we consider $W = 1$ and $W = 4$ and we fix $N = 200$. By examining the compared CDFs, we can see again that our second stage approximation of the CDF provides a more accurate result of the empirical CDF of the FAS channel than the analytical CDF in [1]. Furthermore, we can see that as W varies from 1 to 4, the CDF in [1] remains almost unchanged while the FAS empirical CDF, as well as our approximation show a considerable shift to the right. This indicates that for $N = 200$, increasing the length of the FAS line-space can have a major impact on the probability of outage, which is not captured by the model in [1]. To conclude, these experiments show that, for a fixed N , increasing the spacial separation between the ports by increasing W , and thus decreasing their inter-correlation, can significantly reduce the probability of outage. On the other hand, if we fix W , decreasing the spatial separation between the FAS ports by increasing N , and thus increasing their inter-correlation, does not seem to have a major impact on the probability of outage. These two observations do not match the results given by [1] for the tested values of N and W in fig. 5. Nevertheless, it is important to highlight that we are considering a relatively high density of ports. Indeed, this density does not only depend on the W to N ratio, but it also

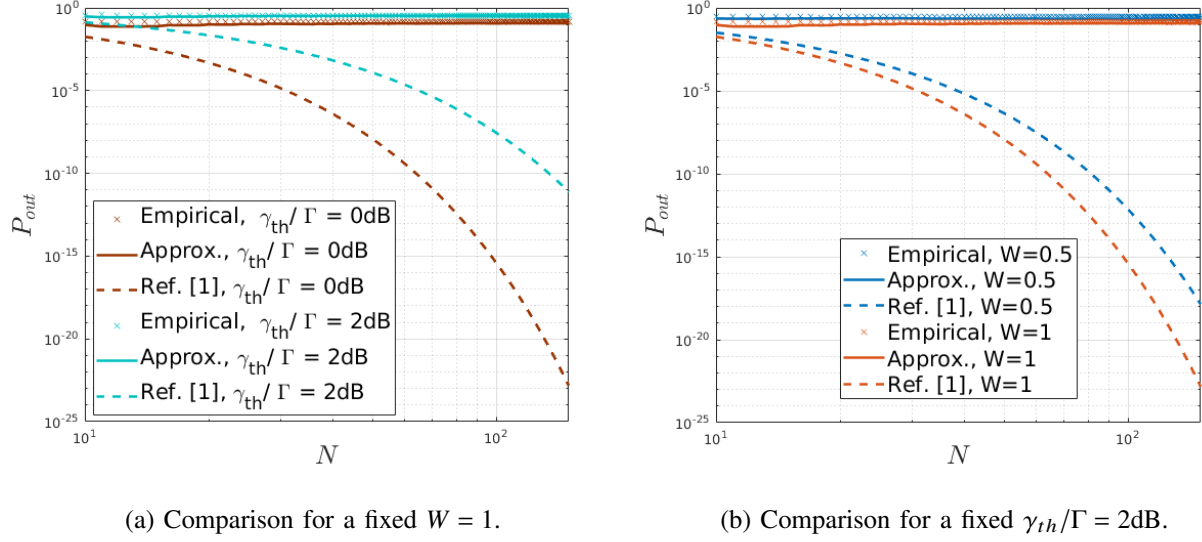


Fig. 6: Probability of outage of the second stage approximation compared to [1].

depends on the wavelength λ , since the inter-ports spacing is $\frac{W\lambda}{N-1}$. According to [1], sub-6GHz is particularly suitable for FAS because the Rayleigh fading model becomes inaccurate for the millimeter-wave bands. If we consider the frequency 5GHz, we will have a port approximately every 1.2 millimeters for $W = 1$, $N = 40$ and $W = 4$, $N = 200$. In the case of $W = 1$, $N = 200$, the inter-antenna spacing can go down to 0.3 millimeters. In these cases, fig. 5, show that the CDF of the FAS [1] fails to match the empirical cdf of the FAS. However, for a few spaced ports, the CDF of the FAS in [1] approaches more the empirical CDF, and it has been shown to be exact for $N = 2$.

c) FAS performance Analysis: to assess the FAS performance for a larger range of N , we plot the outage probability P_{out} versus the number of ports N , for different values of target SNR γ_{th}/Γ , and different values of W . More precisely, in fig. 6, we compare the probability of outage given by the second stage approximation (Approx.) to the one given by equation (16) in [1] (Ref. [1]), and to the empirical probability of outage (Empirical). In fig. 6a, we fix $W = 1$ and we consider two levels of target SNR, 0dB and 2dB. As expected, the probability of outage rises as the SNR target increases. However, the main observation is that the probability of outage of our model accurately approximates the empirical probability of outage, which is considerably high and almost constant compared to the one in [1]. More precisely, if we consider the ambitious SNR target $\gamma_{th}/\Gamma = 0\text{dB}$, both the empirical and approximated probabilities of outage are around

10^{-1} independently of the number of ports N . On the other hand, the probability of outage in [1] starts at 0.01 for $N = 10$, and decreases without a floor to reach $1.52 \cdot 10^{-23}$ for $N = 150$. This shows that parameterizing the channel as in [1] do not accurately capture the correlation between the FAS ports and provides an optimistic performance analysis. The interpretation of this result comes back again to the intuition linking diversity to independent channels. In fact, as N rises for a fixed W , we are reducing the space between the ports, increasing their inter-correlation, and therefore, lowering diversity. This can be shown by a probability of outage that does not scale with N . In fig. 6b, we fix $\gamma_{th}/\Gamma = 0\text{dB}$ and we consider two values of W , 0.5 and 1. As expected, the probability of outage drops as the space increases with W . Further, we can observe the same behavior as in fig. 6a, with an almost constant probability of outage that does continuously drop with N as it is stated in [1]. This again can be explained by the fact that the model used in [1] simplifies the structure of the covariance matrix, and does not fully capture the dependence between the ports as their density increases. In fact, while it ensures that the correlation between the reference port and the other ports follows Jake's model, the other correlations taken between two ports that none of them is the reference port do not follow the covariance function given by Jake's model. Therefore, simplifying the correlation structure of these highly dependent channels can considerably influence the achievable performance analysis. Although, the outage probabilities are still high, the idea of diversity in a small space is still worth exploring. However, it is constrained by space and needs careful analysis to investigate the specific ranges of N and W where we can have a significant gain with respect to traditional multi-antenna systems.

V. CONCLUSION

Fluid antenna systems allow for adopting multiple antennas in a mobile device by exploiting diversity hidden in a small space, and previous related works have revealed considerable performance gain. Nevertheless, assessing the true benefits of such arising technology remains a function of the careful modeling of the FAS channel. It is, however, challenging to model the channel in an analytically tractable manner. Therefore, this work proposes a two stages approximation model of the FAS channel. Unlike previous work in the literature, the proposed approximations closely follow the empirical model. To this end, we believe our approximation offers an accurate look at the achievable performance of FAS under a less-idealized correlation model. The paper first presents the first stage approximation, which considerably reduces the

number of multi-fold integrals in outage probability. Then, for more insight, we provide a second stage approximation representing the probability of outage as a power of a single integral, allowing for more tractability of the model with some trade-off on the accuracy. Finally, our numerical results assess the accuracy of the proposed approximations and compare our work with the previous related work. In our results, we argue that by closely approximating its distribution, the probability of outage of the FAS remains almost constant as N grows. Therefore, our work opens the door for future research to investigate the FAS settings where diversity gain can be guaranteed.

APPENDIX A

On the one hand, the entry of the covariance $\mathbf{\Sigma}_h$ at (i, j) for $i, j \in \{1, \dots, N\}$ is written as

$$(\mathbf{\Sigma}_h)_{i,j} = \begin{cases} \sigma_h^2 & \text{if } i = j \\ \sigma_h^2 \sum_{l=1}^M \alpha_{i,l} \alpha_{j,l} & \text{if } i \neq j. \end{cases} \quad (52)$$

On the other hand, by diagonalizing the covariance matrix $\mathbf{\Sigma}_g$, we can write

$$\mathbf{\Sigma}_g = \mathbf{U} \mathbf{S} \mathbf{U}^T = \sum_{l=1}^N s_l \mathbf{u}_l \mathbf{u}_l^T, \quad (53)$$

where $(s_1, \dots, s_N) = \text{diag}(\mathbf{S})$ are the eigenvalues of $\mathbf{\Sigma}_g$ and $(\mathbf{u}_1, \dots, \mathbf{u}_N) = \mathbf{U}$ are their associated eigenvectors and the columns of \mathbf{U} . Therefore, the entry of $\mathbf{\Sigma}_g$ at (i, j) for $i, j \in \{1, \dots, N\}$ can be written as

$$(\mathbf{\Sigma}_g)_{i,j} = \sum_{l=1}^N s_l u_{i,l} u_{j,l}. \quad (54)$$

For $\sigma_h = \sigma$, $M = N$ and $\alpha_{i,j} = \frac{\sqrt{s_j}}{\sigma} u_{i,j}$, $1 \leq i, j \leq N$, (52) and (54) imply that

$$(\mathbf{\Sigma}_g)_{i,j} = (\mathbf{\Sigma}_h)_{i,j}, \quad \text{for } i, j \in \{1, \dots, N\}. \quad (55)$$

Since \mathbf{g} and \mathbf{h} have the same mean vector according to (9) and the same covariance matrix according to (55), then they have the same joint distribution.

Furthermore, we have

$$\sum_{j=1}^M \alpha_{i,j}^2 = \sum_{j=1}^N \frac{s_j}{\sigma^2} u_{i,j}^2 = 1. \quad (56)$$

Therefore, $\forall k \in \{1, \dots, N\}$,

$$\begin{aligned}
 g_k &\stackrel{d}{=} h_k \\
 &= \sigma \sqrt{1 - \sum_{l=1}^N \alpha_{k,l}^2} (x_k + jy_k) + \sigma \sum_{l=1}^N \alpha_{k,l} (a_l + jb_l) \\
 &= \sum_{l=1}^N \sqrt{s_l} u_{k,l} (a_l + jb_l).
 \end{aligned} \tag{57}$$

APPENDIX B

Let $M = \epsilon$ -rank for $\epsilon > 0$. We have

$$\epsilon\text{-rank} = \max\{l \in \{1, \dots, N\}, s_l \geq \epsilon\}. \tag{58}$$

Therefore,

$$\lim_{\epsilon \rightarrow 0} \epsilon\text{-rank} = N. \tag{59}$$

This means that $\forall k \in \{1, \dots, N\}$,

$$\lim_{\epsilon \rightarrow 0} \sqrt{\sigma^2 - \sum_{l=1}^{\epsilon\text{-rank}} s_l u_{k,l}^2} (x_k + jy_k) + \sum_{l=1}^{\epsilon\text{-rank}} \sqrt{s_l} u_{k,l} (a_l + jb_l) = \sum_{l=1}^N \sqrt{s_l} u_{k,l} (a_l + jb_l), \tag{60}$$

which implies that

$$\hat{g}_k \xrightarrow{d} g_k \text{ as } \epsilon \rightarrow 0, \quad \forall k \in \{1, \dots, N\}. \tag{61}$$

Therefore,

$$\hat{\mathbf{g}} \xrightarrow{d} \mathbf{g} \text{ as } \epsilon \rightarrow 0. \tag{62}$$

APPENDIX C

For $\epsilon > 0$ and $\epsilon\text{-rank} < N$,

$$\hat{g}_k = \sqrt{\sigma^2 - \sum_{l=1}^{\epsilon\text{-rank}} s_l u_{k,l}^2} (x_k + jy_k) + \sum_{l=1}^{\epsilon\text{-rank}} \sqrt{s_l} u_{k,l} (a_l + jb_l), \quad \forall k \in \{1, \dots, N\}. \tag{63}$$

Let \mathbf{a} and \mathbf{b} be the random vectors defined as

$$\mathbf{a} = (a_1, a_2, \dots, a_{\epsilon\text{-rank}})^T, \quad \mathbf{b} = (b_1, b_2, \dots, b_{\epsilon\text{-rank}})^T. \tag{64}$$

We can see that $\hat{g}_1|(\mathbf{a}, \mathbf{b}), \hat{g}_2|(\mathbf{a}, \mathbf{b}), \dots, \hat{g}_N|(\mathbf{a}, \mathbf{b})$ are independent and we have

$$\hat{g}_k|(\mathbf{a}, \mathbf{b}) \sim \mathcal{CN} \left(\sum_{l=1}^{\epsilon\text{-rank}} \sqrt{s_l} u_{k,l} (a_l + j b_l), (\sigma^2 - \sum_{l=1}^{\epsilon\text{-rank}} s_l u_{k,l}^2) \right), \quad \forall k \in \{1, 2, \dots, N\}, \quad (65)$$

which implies that $|g_k| |(\mathbf{a}, \mathbf{b})$ is a Rician distribution [11] and its CDF can be written as

$$F_{|\hat{g}_k| |(\mathbf{a}, \mathbf{b})}(r_k) = 1 - Q_1 \left(\frac{\sqrt{2 \left(\sum_{l=1}^{\epsilon\text{-rank}} \sqrt{s_l} u_{k,l} a_l \right)^2 + 2 \left(\sum_{l=1}^{\epsilon\text{-rank}} \sqrt{s_l} u_{k,l} b_l \right)^2}}{\sqrt{\sigma^2 - \sum_{l=1}^{\epsilon\text{-rank}} s_l u_{k,l}^2}}, \frac{\sqrt{2} r_k}{\sqrt{\sigma^2 - \sum_{l=1}^{\epsilon\text{-rank}} s_l u_{k,l}^2}} \right). \quad (66)$$

By independence, we can write

$$F_{(|\hat{g}_1|, |\hat{g}_2|, \dots, |\hat{g}_N|) |(\mathbf{a}, \mathbf{b})}(r_1, r_2, \dots, r_N) = \prod_{k=1}^N F_{|\hat{g}_k| |(\mathbf{a}, \mathbf{b})}(r_k). \quad (67)$$

Therefore,

$$F_{(|\hat{g}_1|, |\hat{g}_2|, \dots, |\hat{g}_N|) |(\mathbf{a}, \mathbf{b})}(r_1, r_2, \dots, r_N) = \int \dots \int \prod_{k=1}^N F_{|\hat{g}_k| |(\mathbf{a}, \mathbf{b})}(r_k) f_{\mathbf{a}, \mathbf{b}} da_1 \dots da_{\epsilon\text{-rank}} db_1 \dots db_{\epsilon\text{-rank}}, \quad (68)$$

where

$$f_{a,b}(a_1, \dots, a_{\epsilon\text{-rank}}, b_1, \dots, b_{\epsilon\text{-rank}}) = \prod_{l=1}^{\epsilon\text{-rank}} \frac{1}{\pi} \exp(-(a_l^2 + b_l^2)). \quad (69)$$

Finally, we get the expression in (16) by plugging $f_{a,b}$ and $F_{|\hat{g}_k| |(\mathbf{a}, \mathbf{b})}(r_k)$ in (68).

APPENDIX D

We have \mathbf{T}_N of size $N \times N$ such that, for $k, \ell \in \{1, \dots, N\}$ and $0 < c < \frac{1}{2}$,

$$\begin{aligned} (\mathbf{T}_N)_{(k,\ell)} &= \sigma^2 J_0(2\pi(k-\ell)c) \\ &= \frac{\sigma^2}{2\pi} \int_{-\pi}^{\pi} e^{i2\pi(k-\ell)c \sin(\tau)} d\tau. \end{aligned} \quad (70)$$

We consider the following Fourier transform pair,

$$\hat{f}(\lambda) = \sum_{k=-\infty}^{\infty} \sigma^2 J_0(2\pi k c) e^{ik\lambda}; \lambda \in [-\pi, \pi]. \quad (71)$$

$$\sigma^2 J_0(2\pi k c) = \frac{1}{2\pi} \int_{-\pi}^{\pi} \hat{f}(\lambda) e^{-ik\lambda} d\lambda. \quad (72)$$

Therefore,

$$\begin{aligned}
\hat{f}(\lambda) &= \sum_{k=-\infty}^{\infty} \frac{\sigma^2}{2\pi} \int_{-\pi}^{\pi} e^{i2\pi k c \sin(\tau)} d\tau e^{ik\lambda} \\
&= \frac{\sigma^2}{2\pi} \int_{-\pi}^{\pi} \sum_{k=-\infty}^{\infty} e^{i2\pi k (c \sin(\tau) + \frac{\lambda}{2\pi})} d\tau \\
&= \frac{\sigma^2}{2\pi} \int_{-\pi}^{\pi} \sum_{n=-\infty}^{\infty} \delta(c \sin(\tau) + \frac{\lambda}{2\pi} - n) d\tau \text{ (by the Poisson sum formula [30])}.
\end{aligned} \tag{73}$$

For $\delta(c \sin(\tau) + \frac{\lambda}{2\pi} - n)$ to be non zero, we need $c \sin(\tau) + \frac{\lambda}{2\pi} - n$ to be zero. Thus,

$$c \sin(\tau) + \frac{\lambda}{2\pi} - n = 0 \Rightarrow \sin(\tau) = \frac{1}{c} \left(n - \frac{\lambda}{2\pi} \right) \tag{74}$$

$$\Rightarrow -1 \leq \frac{1}{c} \left(n - \frac{\lambda}{2\pi} \right) \leq 1 \tag{75}$$

$$\Rightarrow \frac{\lambda}{2\pi} - c \leq n \leq \frac{\lambda}{2\pi} + c. \tag{76}$$

Since $0 < c < \frac{1}{2}$ and $-\pi \leq \lambda \leq \pi$, then $\frac{\lambda}{2\pi} + c < 1$ and $\frac{\lambda}{2\pi} - c > -1$. Therefore, the only integer n that can verify (76) is zero. Therefore,

$$\hat{f}(\lambda) = \frac{\sigma^2}{2\pi} \int_{-\pi}^{\pi} \delta(c \sin(\tau) + \frac{\lambda}{2\pi}) d\tau \mathbf{1}_{\{0 \in [\frac{\lambda}{2\pi} - c, \frac{\lambda}{2\pi} + c]\}}. \tag{77}$$

By using the identity [31], $\delta(\Phi(\tau)) = \sum_j \frac{1}{|\Phi'(\tau_j)|} \delta(\tau - \tau_j)$ where τ_j is such $\Phi(\tau_j) = 0$ and $\Phi'(\tau_j) \neq 0$, we can write

$$\hat{f}(\lambda) = \frac{2\sigma^2}{\sqrt{(2\pi c)^2 - \lambda^2}} \mathbf{1}_{\{-2\pi c \leq \lambda \leq 2\pi c\}}. \tag{78}$$

By applying the result from [32], corollary 5, we can write

$$\begin{aligned}
D(x) &= \frac{1}{2\pi} \int_{\hat{f}(\lambda) \leq x} d\lambda \\
&= \frac{1}{2\pi} \int_{-\pi}^{\pi} \mathbf{1}_{\{\hat{f}(\lambda) \leq x\}} d\lambda \\
&= \frac{1}{2\pi} \int_{-\pi}^{-2\pi c} \mathbf{1}_{\{0 \leq x\}} d\lambda + \frac{1}{2\pi} \int_{-2\pi c}^{2\pi c} \mathbf{1}_{\{\frac{2\sigma^2}{\sqrt{(2\pi c)^2 - \lambda^2}} \leq x\}} d\lambda + \frac{1}{2\pi} \int_{2\pi c}^{\pi} \mathbf{1}_{\{0 \leq x\}} d\lambda \\
&= \begin{cases} 1 - 2c & \text{if } 0 < x < \frac{\sigma^2}{\pi c} \\ 1 - 2c + \sqrt{(2c)^2 - \frac{4\sigma^4}{(\pi x)^2}} & \text{if } x \geq \frac{\sigma^2}{\pi c}. \end{cases}
\end{aligned} \tag{79}$$

APPENDIX E

1) Let $r \in \{1, \dots, R\}$ and $(\hat{g}_{1,r}, \dots, \hat{g}_{N,r})^T$ be the r -th column of $\hat{\mathbf{G}}$. we have

$$E[(\hat{g}_{1,r}, \dots, \hat{g}_{N,r})^T] = E[(\hat{g}_1, \dots, \hat{g}_N)^T] = (0, \dots, 0)^T, \quad (80)$$

$$\text{Cov}[\hat{g}_{i,r}, \hat{g}_{j,r}] = \text{Cov}[\hat{g}_i, \hat{g}_j] = \begin{cases} \sigma^2 & \text{if } i = j \\ \sum_{l=1}^{\epsilon\text{-rank}} s_l u_{i,l} u_{j,l} & \text{if } i \neq j. \end{cases} \quad (81)$$

Therefore, $(\hat{g}_{1,r}, \dots, \hat{g}_{N,r})^T$ and $(\hat{g}_1, \dots, \hat{g}_N)^T$ have the same joint distribution $\forall r \in \{1, \dots, R\}$.

2) Let $r, p \in \{1, \dots, R\}$, such that $r \neq p$. For the r -th and p -th columns of $\hat{\mathbf{G}}$, we have

$$\text{Cov}[\hat{g}_{k,r}, \hat{g}_{l,p}] = 0, \quad \forall k, p \in \{1, \dots, N\}. \quad (82)$$

Therefore, $(\hat{g}_{1,r}, \dots, \hat{g}_{N,r})^T$ and $(\hat{g}_{1,p}, \dots, \hat{g}_{N,p})^T$ are independent, and thus, all the columns of $\hat{\mathbf{G}}$.

3) Let $k, l \in \{1, \dots, N\}$, such that $k \neq l$. For the k -th and l -th rows of $\hat{\mathbf{G}}$, we have according to equation (81)

$$\text{Cov}[\hat{g}_{k,r}, \hat{g}_{l,r}] \neq 0, \quad \forall r \in \{1, \dots, R\}. \quad (83)$$

Therefore, $(\hat{g}_{k,1}, \dots, \hat{g}_{k,R})$ and $(\hat{g}_{l,1}, \dots, \hat{g}_{l,R})$ are dependent, and thus, all the rows of $\hat{\mathbf{G}}$.

APPENDIX F

We can see that $E(\hat{g}_{k,r}) = 0$ for all $k \in \{1, \dots, N\}$ and $r \in \{1, \dots, R\}$. Furthermore, for $i, j \in \{1, \dots, N\}$ and $m, n \in \{1, \dots, R\}$,

$$(\Sigma_{\hat{\mathbf{G}}})_{i,j}^{m,n} = \text{Cov}(\hat{g}_{i,m}, \hat{g}_{j,n}) = \begin{cases} 0 & \text{if } m \neq n \\ \sigma^2 & \text{if } i = j \text{ and } m = n \\ \sum_{l=1}^{\epsilon\text{-rank}} s_l u_{i,l} u_{j,l} & \text{if } i \neq j \text{ and } m = n, \end{cases} \quad (84)$$

where $(\Sigma_{\hat{\mathbf{G}}})_{i,j}^{m,n}$ is the entry (i, j) in the block (m, n) of $\Sigma_{\hat{\mathbf{G}}}$. Therefore, the result in equation

(31) follows directly from the expression of the covariance matrix of $\hat{\mathbf{g}}$ written as

$$(\Sigma_{\hat{\mathbf{g}}})_{i,j} = \begin{cases} \sigma^2 & \text{if } i = j \\ \sum_{l=1}^{\epsilon\text{-rank}} s_l u_{i,l} u_{j,l} & \text{if } i \neq j \end{cases} \quad \text{for } i, j \in \{1, \dots, N\}. \quad (85)$$

APPENDIX G

1) Let $r \in \{1, \dots, R\}$ and $(\tilde{g}_{1,r}, \dots, \tilde{g}_{N,r})^T$ be the r -th column of $\tilde{\mathbf{G}}$. we have

$$E[(\tilde{g}_{1,r}, \dots, \tilde{g}_{N,r})^T] = E[(\tilde{g}_1, \dots, \tilde{g}_N)^T] = (0, \dots, 0)^T, \quad (86)$$

$$\text{Cov}[\tilde{g}_{i,r}, \tilde{g}_{j,r}] = \text{Cov}[\tilde{g}_i, \tilde{g}_j] = \begin{cases} \sigma^2 & \text{if } i = j \\ 0 & \text{if } i \neq j. \end{cases} \quad (87)$$

Therefore, $(\tilde{g}_{1,r}, \dots, \tilde{g}_{N,r})^T$ and $(\tilde{g}_1, \dots, \tilde{g}_N)^T$ have the same joint distribution $\forall r \in \{1, \dots, R\}$.

2) Let $r, p \in \{1, \dots, R\}$, such that $r \neq p$. For the r -th and p -th columns of $\tilde{\mathbf{G}}$, we have

$$\text{Cov}(\tilde{g}_{k,r}, \tilde{g}_{k,p}) = \begin{cases} \sigma^2 & \text{if } r = p \\ \sum_{l=1}^{\epsilon\text{-rank}} s_l u_{k,l}^2 & \text{if } r \neq p \end{cases} \neq 0, \quad \forall k \in \{1, \dots, N\}. \quad (88)$$

Therefore, the columns $(\tilde{g}_{1,r}, \dots, \tilde{g}_{N,r})^T$ and $(\tilde{g}_{1,p}, \dots, \tilde{g}_{N,p})^T$ are dependent for $r \neq p$, and thus, all the columns of $\tilde{\mathbf{G}}$.

3) Let $k, l \in \{1, \dots, N\}$, such that $k \neq l$. For the l -th and k -th rows of $\tilde{\mathbf{G}}$, we have

$$\text{Cov}[\tilde{g}_{k,r}, \tilde{g}_{l,p}] = 0 \quad \forall r, p \in \{1, \dots, R\}. \quad (89)$$

Therefore, the rows $(\tilde{g}_{k,1}, \dots, \tilde{g}_{k,R})$ and $(\tilde{g}_{l,1}, \dots, \tilde{g}_{l,R})$ are independent for $k \neq l$, and thus, all the rows of $\tilde{\mathbf{G}}$.

APPENDIX H

We can see that $E(\tilde{g}_{k,r}) = 0$ for all $k \in \{1, \dots, N\}$ and $r \in \{1, \dots, R\}$. Furthermore, for $i, j \in \{1, \dots, R\}$ and $m, n \in \{1, \dots, N\}$,

$$\begin{aligned} (\Sigma_{\tilde{\mathbf{G}}})_{i,j}^{m,n} &= \text{Cov}(\tilde{g}_{m,i}, \tilde{g}_{n,j}) \\ &= \begin{cases} 0 & \text{if } m \neq n \\ \sigma^2 & \text{if } i = j \text{ and } m = n \\ \sum_{l=1}^{\epsilon\text{-rank}} s_l u_{n,l}^2 & \text{if } i \neq j \text{ and } m = n, \end{cases} \end{aligned} \quad (90)$$

where $(\Sigma_{\hat{\mathbf{G}}})_{i,j}^{m,n}$ is the entry (i, j) in the block (m, n) of $\Sigma_{\hat{\mathbf{G}}}$. Therefore, the result in equation (39) follows directly from taking the matrix Σ_k , for $k \in \{1, \dots, N\}$ as

$$(\Sigma_k)_{i,j} = \begin{cases} \sigma^2 & \text{if } i = j \\ \sum_{l=1}^{\epsilon\text{-rank}} s_l u_{k,l}^2 & \text{if } i \neq j \end{cases} \quad \text{for } i, j \in \{1, \dots, R\}. \quad (91)$$

APPENDIX I

We have Ψ_R defined as

$$\Psi_R = \max\{|\tilde{g}_{k,r}|, 1 \leq k \leq N, 1 \leq r \leq R\}. \quad (92)$$

Therefore,

$$\begin{aligned} F_{\Psi_R}(g) &= P(\max_{1 \leq k \leq N} \{ \max_{1 \leq r \leq R} \{|\tilde{g}_{k,r}|\} \} \leq g) \\ &= \prod_{k=1}^N P(\max_{1 \leq r \leq R} \{|\tilde{g}_{k,r}|\} \leq g) \quad (\text{given by the independence property in corollary III.9.1}) \\ &= \prod_{k=1}^N E_{\mathbf{a}^{(k)}, \mathbf{b}^{(k)}} \left[P(\max_{1 \leq r \leq R} \{|\tilde{g}_{k,r}|\} |(\mathbf{a}^{(k)}, \mathbf{b}^{(k)})\} \leq g) \right], \end{aligned} \quad (93)$$

where $\mathbf{a}^{(k)} = (a_{1,k}, a_{2,k}, \dots, a_{\epsilon\text{-rank},k})^T$, $\mathbf{b}^{(k)} = (b_{1,k}, b_{2,k}, \dots, b_{\epsilon\text{-rank},k})^T$ and $E_{\mathbf{a}^{(k)}, \mathbf{b}^{(k)}}[\cdot]$ is the expectation with respect to the random variable $(\mathbf{a}^{(k)}, \mathbf{b}^{(k)})$. From the expression of $\tilde{g}_{k,r}$ given in definition III.4, we can see that $\tilde{g}_{k,1}|(\mathbf{a}^{(k)}, \mathbf{b}^{(k)})$, $\tilde{g}_{k,2}|(\mathbf{a}^{(k)}, \mathbf{b}^{(k)})$, \dots , $\tilde{g}_{k,R}|(\mathbf{a}^{(k)}, \mathbf{b}^{(k)})$ are independent and identically distributed. Further, for $k \in \{1, \dots, N\}$,

$$\tilde{g}_{k,r}|(\mathbf{a}^{(k)}, \mathbf{b}^{(k)}) \sim \mathcal{CN}(\sum_{l=1}^{\epsilon\text{-rank}} \sqrt{s_l} u_{k,l} (a_{l,k} + j b_{l,k}), \sigma^2 - \sum_{l=1}^{\epsilon\text{-rank}} s_l u_{k,l}^2), \quad \forall r \in \{1, \dots, R\}. \quad (94)$$

This implies that $|\tilde{g}_{k,r}| |(\mathbf{a}^{(k)}, \mathbf{b}^{(k)})$ is Rician distributed [11], and its CDF can be written as

$$F_{|\tilde{g}_{k,r}| |(\mathbf{a}^{(k)}, \mathbf{b}^{(k)})}(g) = 1 - Q_1 \left(\frac{\sqrt{2 \left(\sum_{l=1}^{\epsilon\text{-rank}} \sqrt{s_l} u_{k,l} a_{l,k} \right)^2 + 2 \left(\sum_{l=1}^{\epsilon\text{-rank}} \sqrt{s_l} u_{k,l} b_{l,k} \right)^2}}{\sqrt{\sigma^2 - \sum_{l=1}^{\epsilon\text{-rank}} s_l u_{k,l}^2}}, \frac{\sqrt{2}g}{\sqrt{\sigma^2 - \sum_{l=1}^{\epsilon\text{-rank}} s_l u_{k,l}^2}} \right). \quad (95)$$

Therefore,

$$\begin{aligned} P(\max_{1 \leq r \leq R} \{|\tilde{g}_{k,r}| |(\mathbf{a}^{(k)}, \mathbf{b}^{(k)})\} \leq g) &= \prod_{r=1}^R P(|\tilde{g}_{k,r}| |(\mathbf{a}^{(k)}, \mathbf{b}^{(k)}) \leq g) \quad (\text{independence}) \\ &= \left[P(|\tilde{g}_{k,r}| |(\mathbf{a}^{(k)}, \mathbf{b}^{(k)}) \leq g) \right]^R \quad (\text{identical distribution}) \quad (96) \\ &= \left[F_{|\tilde{g}_{k,r}| |(\mathbf{a}^{(k)}, \mathbf{b}^{(k)})}(g) \right]^R. \end{aligned}$$

Furthermore,

$$f_{\mathbf{a}^{(k)}, \mathbf{b}^{(k)}}(a_{1,k}, \dots, a_{\epsilon\text{-rank},k}, b_{1,k}, \dots, b_{\epsilon\text{-rank},k}) = \prod_{l=1}^{\epsilon\text{-rank}} \frac{1}{\pi} \exp(-(a_{l,k}^2 + b_{l,k}^2)). \quad (97)$$

Therefore, we can write

$$E_{\mathbf{a}^{(k)}, \mathbf{b}^{(k)}} \left[P(\max_{1 \leq r \leq R} \{|\tilde{g}_k^{(r)}| \mid (\mathbf{a}^{(k)}, \mathbf{b}^{(k)})\} \leq g) \right] = \int \cdots \int \prod_{l=1}^{\epsilon\text{-rank}} \frac{1}{\pi} \exp(-(a_{l,k}^2 + b_{l,k}^2))$$

$$\left[1 - Q_1 \left(\frac{\sqrt{2 \left(\sum_{l=1}^{\epsilon\text{-rank}} \sqrt{s_l} u_{k,l} a_{l,k} \right)^2 + 2 \left(\sum_{l=1}^{\epsilon\text{-rank}} \sqrt{s_l} u_{k,l} b_{l,k} \right)^2}}{\sqrt{\sigma^2 - \sum_{l=1}^{\epsilon\text{-rank}} s_l u_{k,l}^2}}, \frac{\sqrt{2}g}{\sqrt{\sigma^2 - \sum_{l=1}^{\epsilon\text{-rank}} s_l u_{k,l}^2}} \right) \right]^R \quad (98)$$

$$da_{1,k}, \dots, da_{\epsilon\text{-rank},k}, db_{1,k}, \dots, db_{\epsilon\text{-rank},k}$$

$$= E_{(\mathbf{a}, \mathbf{b})} \left[\left[1 - Q_1 \left(\frac{\sqrt{2 \left(\sum_{l=1}^{\epsilon\text{-rank}} \sqrt{s_l} u_{k,l} a_l \right)^2 + 2 \left(\sum_{l=1}^{\epsilon\text{-rank}} \sqrt{s_l} u_{k,l} b_l \right)^2}}{\sqrt{\sigma^2 - \sum_{l=1}^{\epsilon\text{-rank}} s_l u_{k,l}^2}}, \frac{\sqrt{2}g}{\sqrt{\sigma^2 - \sum_{l=1}^{\epsilon\text{-rank}} s_l u_{k,l}^2}} \right) \right]^R \right],$$

because $(\mathbf{a}^{(k)}, \mathbf{b}^{(k)})$ is identically distributed as (\mathbf{a}, \mathbf{b}) .

On the other hand, we define the random variable Z_k as:

$$Z_k = \left(\sum_{l=1}^{\epsilon\text{-rank}} \sqrt{s_l} u_{k,l} a_l \right)^2 + \left(\sum_{l=1}^{\epsilon\text{-rank}} \sqrt{s_l} u_{k,l} b_l \right)^2$$

$$= \mathbf{a}^T \boldsymbol{\gamma}_k^T \boldsymbol{\gamma}_k \mathbf{a} + \mathbf{b}^T \boldsymbol{\gamma}_k^T \boldsymbol{\gamma}_k \mathbf{b} \quad (99)$$

$$= Z_k^{(a)} + Z_k^{(b)},$$

where $Z_k^{(a)} = \mathbf{a}^T \boldsymbol{\gamma}_k^T \boldsymbol{\gamma}_k \mathbf{a}$, $Z_k^{(b)} = \mathbf{b}^T \boldsymbol{\gamma}_k^T \boldsymbol{\gamma}_k \mathbf{b}$ and $\boldsymbol{\gamma}_k = (\sqrt{s_1} u_{k,1}, \sqrt{s_2} u_{k,2}, \dots, \sqrt{s_{\epsilon\text{-rank}}} u_{k,\epsilon\text{-rank}})$. We would like to determine the distribution of Z_k . First, we have that

$$Z_k^{(a)} = \mathbf{a}^T \boldsymbol{\gamma}_k^T \boldsymbol{\gamma}_k \mathbf{a}$$

$$= \boldsymbol{\gamma}_k \boldsymbol{\gamma}_k^T \left(\mathbf{a}^T \frac{\boldsymbol{\gamma}_k^T \boldsymbol{\gamma}_k}{\boldsymbol{\gamma}_k \boldsymbol{\gamma}_k^T} \mathbf{a} \right) \quad (100)$$

$$= (\sqrt{\boldsymbol{\gamma}_k \boldsymbol{\gamma}_k^T} \mathbf{a}^T) \mathbf{P}_k (\sqrt{\boldsymbol{\gamma}_k \boldsymbol{\gamma}_k^T} \mathbf{a}^T)^T,$$

where $\mathbf{P}_k = \frac{\boldsymbol{\gamma}_k^T \boldsymbol{\gamma}_k}{\boldsymbol{\gamma}_k \boldsymbol{\gamma}_k^T}$ is a projector of rank 1. Therefore, $Z_k^{(a)} \sim \chi^2(1)$ and $f_{Z_k^{(a)}}(z) = \frac{1}{\sqrt{\pi \boldsymbol{\gamma}_k \boldsymbol{\gamma}_k^T} z} \exp(-\frac{z}{\boldsymbol{\gamma}_k \boldsymbol{\gamma}_k^T})$.

Therefore, the pdf of Z_k can be written as:

$$f_{Z_k}(z) = f_{Z_k^{(a)}}(z) * f_{Z_k^{(b)}}(z) = \frac{1}{\boldsymbol{\gamma}_k \boldsymbol{\gamma}_k^T} \exp\left(-\frac{z}{\boldsymbol{\gamma}_k \boldsymbol{\gamma}_k^T}\right), \quad z > 0. \quad (101)$$

Finally, we can write the CDF of Ψ_R as

$$\begin{aligned}
F_{\Psi_R}(g) &= \prod_{k=1}^N E_{\mathbf{a}^{(k)}, \mathbf{b}^{(k)}} \left[P(\max_{1 \leq r \leq R} \{|\tilde{g}_{k,r}|\} | (\mathbf{a}^{(k)}, \mathbf{b}^{(k)}) \} \leq g) \right] \quad (\text{by equation (93)}) \\
&= \prod_{k=1}^N E_{(\mathbf{a}, \mathbf{b})} \left[\left[1 - Q_1 \left(\frac{\sqrt{2 \left(\sum_{l=1}^{\epsilon\text{-rank}} \sqrt{s_l} u_{k,l} a_l \right)^2 + 2 \left(\sum_{l=1}^{\epsilon\text{-rank}} \sqrt{s_l} u_{k,l} b_l \right)^2}}{\sqrt{\sigma^2 - \sum_{l=1}^{\epsilon\text{-rank}} s_l u_{k,l}^2}}, \frac{\sqrt{2}g}{\sqrt{\sigma^2 - \sum_{l=1}^{\epsilon\text{-rank}} s_l u_{k,l}^2}} \right) \right]^R \right] \\
&= \prod_{k=1}^N E_{Z_k} \left[\left[1 - Q_1 \left(\frac{\sqrt{2Z_k}}{\sqrt{\sigma^2 - \sum_{l=1}^{\epsilon\text{-rank}} s_l u_{k,l}^2}}, \frac{\sqrt{2}g}{\sqrt{\sigma^2 - \sum_{l=1}^{\epsilon\text{-rank}} s_l u_{k,l}^2}} \right) \right]^R \right] \\
&= \prod_{k=1}^N \int_0^{+\infty} \frac{1}{\sum_{l=1}^{\epsilon\text{-rank}} s_l u_{k,l}^2} \exp \left(-\frac{r}{\sum_{l=1}^{\epsilon\text{-rank}} s_l u_{k,l}^2} \right) \left[1 - Q_1 \left(\frac{\sqrt{2r}}{\sqrt{\sigma^2 - \sum_{l=1}^{\epsilon\text{-rank}} s_l u_{k,l}^2}}, \frac{\sqrt{2}g}{\sqrt{\sigma^2 - \sum_{l=1}^{\epsilon\text{-rank}} s_l u_{k,l}^2}} \right) \right]^R dr.
\end{aligned} \tag{102}$$

APPENDIX J

By the definitions of the matrices $\Sigma_{\tilde{G}}(R)$ and $\mathbb{I}(R)$, we can write

$$\begin{aligned}
\|\sigma^2 \mathbb{I}(R) - \Sigma_{\tilde{G}}(R)\|_1 &= \max_{1 \leq k \leq N} \|\sigma^2 \mathbf{1}_{R \times R} - \Sigma_k\|_1 \\
&= \max_{1 \leq k \leq N} (R-1)(\sigma^2 - \sum_{l=1}^{\epsilon\text{-rank}} s_l u_{k,l}^2) \\
&\leq \max_{1 \leq k \leq N} N(\sigma^2 - \sum_{l=1}^{\epsilon\text{-rank}} s_l u_{k,l}^2) \quad (\text{for } R \leq N) \\
&\leq \max_{1 \leq k \leq N} N \left(\sum_{l=1}^N s_l u_{k,l}^2 - \sum_{l=1}^{\epsilon\text{-rank}} s_l u_{k,l}^2 \right) \quad (\text{because } \sum_{l=1}^N s_l u_{k,l}^2 = \sigma^2) \\
&\leq \max_{1 \leq k \leq N} N \sum_{l=1+\epsilon\text{-rank}}^N s_l u_{k,l}^2 \\
&\leq \max_{1 \leq k \leq N} N \sum_{l=1+\epsilon\text{-rank}}^N \epsilon u_{k,l}^2 \quad (\text{by definition of } \epsilon\text{-rank}) \\
&\leq N\epsilon \quad (\text{because } \sum_{l=1+\epsilon\text{-rank}}^N u_{k,l}^2 < 1).
\end{aligned} \tag{103}$$

Therefore, for $\epsilon = \frac{\epsilon'}{2N}$,

$$\|\sigma^2 \mathbb{I}(R) - \Sigma_{\tilde{G}}(R)\|_1 \leq \frac{\epsilon'}{2}. \quad (104)$$

On the other hand, by the definition of Σ_G and $\Sigma_{\hat{G}}$, we can write

$$\|\Sigma_{\hat{G}} - \Sigma_G\|_1 = \|\Sigma_{\hat{g}} - \Sigma_g\|_1. \quad (105)$$

Moreover, for $i, j \in \{1, \dots, N\}$, we have

$$(\Sigma_g)_{i,j} = \sum_{l=1}^N s_l u_{i,l} u_{j,l}, \quad (106)$$

$$(\Sigma_{\hat{g}})_{i,j} = \begin{cases} \sum_{l=1}^N s_l u_{i,l}^2 & \text{if } i = j \\ \sum_{l=1}^{\epsilon\text{-rank}} s_l u_{i,l} u_{j,l} & \text{if } i \neq j \end{cases}. \quad (107)$$

We define the matrix Σ' such that for $i, j \in \{1, \dots, N\}$,

$$(\Sigma')_{i,j} = \sum_{l=1}^{\epsilon\text{-rank}} s_l u_{i,l} u_{j,l}. \quad (108)$$

We consider the max norm $\|\cdot\|_{\max}$ and the spectral norm $\|\cdot\|_2$ defined for a matrix \mathbf{A} of size $N \times N$ as follows:

$$\|\mathbf{A}\|_{\max} = \max_{1 \leq i, j \leq N} |a_{i,j}|, \quad \|\mathbf{A}\|_2 = \sigma_{\max}(\mathbf{A}). \quad (109)$$

where $\sigma_{\max}(\mathbf{A})$ is the maximum singular value of \mathbf{A} . we can see that

$$\|\Sigma_g - \Sigma_{\hat{g}}\|_{\max} \leq \|\Sigma_g - \Sigma'\|_{\max}, \quad (110)$$

because while $\Sigma_g - \Sigma_{\hat{g}}$ and $\Sigma_g - \Sigma'$ have the same off-diagonal elements, $\Sigma_g - \Sigma_{\hat{g}}$ has zeros as diagonal elements and $\Sigma_g - \Sigma' = \sum_{l=R+1}^N s_l \mathbf{u}_l \mathbf{u}_l^T$ has positive diagonal elements. Therefore,

$$\begin{aligned} \|\Sigma_g - \Sigma_{\hat{g}}\|_{\max} &\leq \|\Sigma_g - \Sigma'\|_{\max} \\ &\leq \left\| \sum_{l=1+\epsilon\text{-rank}}^N s_l \mathbf{u}_l \mathbf{u}_l^T \right\|_{\max} \\ &\leq \left\| \sum_{l=1+\epsilon\text{-rank}}^N s_l \mathbf{u}_l \mathbf{u}_l^T \right\|_2 \quad (\text{matrix norm equivalence [33]}) \\ &\leq s_{1+\epsilon\text{-rank}} \\ &\leq \epsilon. \end{aligned} \quad (111)$$

This means that,

$$\|\Sigma_{\hat{G}} - \Sigma_G\|_1 = \|\Sigma_{\hat{g}} - \Sigma_g\|_1 \quad (112)$$

$$\leq N\epsilon \text{ (using the result from equation (111)).} \quad (113)$$

Therefore, for $\epsilon = \frac{\epsilon'}{2N}$,

$$\|\Sigma_{\hat{G}} - \Sigma_G\|_1 \leq \frac{\epsilon'}{2}. \quad (114)$$

By combining equations (114) and (104), we get

$$\left| \|\Sigma_{\hat{G}}(R) - \Sigma_{\hat{G}}(R)\|_1 - \|\Sigma_G(R) - \sigma^2 \mathbb{I}(R)\|_1 \right| \leq \|\Sigma_{\hat{G}}(R) - \Sigma_{\hat{G}}(R) - \Sigma_G(R) + \sigma^2 \mathbb{I}(R)\|_1 \quad (115)$$

$$\leq \|\Sigma_{\hat{G}}(R) - \Sigma_G(R)\|_1 + \|\sigma^2 \mathbb{I}(R) - \Sigma_{\hat{G}}(R)\|_1 \quad (116)$$

$$\leq \frac{\epsilon'}{2} + \frac{\epsilon'}{2} \quad (117)$$

$$\leq \epsilon'. \quad (118)$$

APPENDIX K

We have

$$\Sigma_G(R) = \begin{pmatrix} \Sigma_g & 0 & \cdots & 0 \\ 0 & \Sigma_g & \cdots & 0 \\ \vdots & \vdots & \ddots & \vdots \\ 0 & 0 & \cdots & \Sigma_g \end{pmatrix} \quad \mathbb{I}(R) = \begin{pmatrix} \mathbf{1}_{R \times R} & 0 & \cdots & 0 \\ 0 & \mathbf{1}_{R \times R} & \cdots & 0 \\ \vdots & \vdots & \ddots & \vdots \\ 0 & 0 & \cdots & \mathbf{1}_{R \times R} \end{pmatrix}, \quad (119)$$

We can see that $\Sigma_G(R)$ is a block diagonal matrix with R equal blocks, each of size $N \times N$. On the other hand, $\mathbb{I}(R)$ is a block matrix with N equal blocks, each of size $R \times R$. Then, both matrices $\Sigma_G(R)$ and $\mathbb{I}(R)$ are of size $NR \times NR$. Furthermore, for R divisor of N , $\Sigma_G(R) - \sigma^2 \mathbb{I}(R)$ is block diagonal with R equal blocks, each of size $N \times N$. More specifically, one of the diagonal blocks of the matrix $\Sigma_G(R) - \sigma^2 \mathbb{I}(R)$, say the first block, is written as

$$(\Sigma_G(R) - \sigma^2 \mathbb{I}(R))^{1,1} = \Sigma_g - \sigma^2 \underbrace{\text{diag}(\mathbf{1}_{R \times R}, \dots, \mathbf{1}_{R \times R})}_{\frac{N}{R} \text{ times}}. \quad (120)$$

In other words, by examining one of the diagonal blocks of the matrix $(\Sigma_G(R) - \sigma^2 \mathbb{I}(R))$, we can see that R determines the size of diagonal blocks of Σ_g from which σ^2 is subtracted.

Further, we have

$$(\Sigma_g)_{k,\ell} = \sigma^2 J_0 \left(\frac{2\pi(k-\ell)}{N-1} W \right), \text{ for } \ell, k \in \{1, \dots, N\}. \quad (121)$$

Therefore, if we denote by $(\Sigma_G(R) - \sigma^2 \mathbb{I}(R))_{k,\ell}^{m,n}$ the entry (k, ℓ) in the block (m, n) of the matrix $(\Sigma_G(R) - \sigma^2 \mathbb{I}(R))$ with $1 \leq m, n \leq R$ and $1 \leq k, \ell \leq N$, then we can write

$$(\Sigma_G(R) - \sigma^2 \mathbb{I}(R))_{k,\ell}^{m,n} = \begin{cases} \sigma^2 \left(J_0 \left(\frac{2\pi(k-\ell)}{N-1} W \right) - 1 \right) & \text{if } m = n \text{ and } (k, \ell) \in S \\ \sigma^2 J_0 \left(\frac{2\pi(k-\ell)}{N-1} W \right) & \text{if } m = n \text{ and } (k, \ell) \notin S \\ 0 & \text{otherwise,} \end{cases} \quad (122)$$

where S is defined as

$$S = \{(k, \ell) \in \mathbb{N}, \exists p \in \{0, \dots, \frac{N}{R} - 1\}, \text{ such that } pR + 1 \leq k, \ell \leq (p+1)R\}.$$

Therefore, the norm 1 of the matrix $(\Sigma_G(R) - \sigma^2 \mathbb{I}(R))$ is equal to the norm 1 of one of its blocks (all its blocks are equal) and we can write

$$\begin{aligned} \|\Sigma_G(R) - \sigma^2 \mathbb{I}(R)\|_1 &= \|(\Sigma_G(R) - \sigma^2 \mathbb{I}(R))^{1,1}\|_1 \\ &= \left\| \Sigma_g - \sigma^2 \underbrace{\text{diag}(\mathbf{1}_{R \times R}, \dots, \mathbf{1}_{R \times R})}_{\frac{N}{R} \text{ times}} \right\|_1 \\ &= \max_{0 \leq p \leq \frac{N}{R} - 1} \max_{pR+1 \leq \ell \leq (p+1)R} \sum_{k=1}^{pR} \sigma^2 \left| J_0 \left(\frac{2\pi(k-\ell)}{N-1} W \right) \right| \\ &\quad + \sum_{k=pR+1}^{(p+1)R} \sigma^2 \left| J_0 \left(\frac{2\pi(k-\ell)}{N-1} W \right) - 1 \right| \\ &\quad + \sum_{k=pR+R+1}^N \sigma^2 \left| J_0 \left(\frac{2\pi(k-\ell)}{N-1} W \right) \right|. \end{aligned} \quad (123)$$

To solve (P3), we would like to find R_3^* , a divisor of N , that minimizes $\|\Sigma_G(R) - \sigma^2 \mathbb{I}(R)\|_1$ given by the expression above. We can see that increasing R increases the size of the diagonal blocks of Σ_g from which σ^2 is subtracted. However, this does not necessarily decrease the maximum absolute column sum of the matrix $\Sigma_g - \sigma^2 \underbrace{\text{diag}(\mathbf{1}_{R \times R}, \dots, \mathbf{1}_{R \times R})}_{\frac{N}{R} \text{ times}}$. In fact, increasing

R decreases the norm 1 of the matrix $\Sigma_g - \sigma^2 \underbrace{\text{diag}(\mathbf{1}_{R \times R}, \dots, \mathbf{1}_{R \times R})}_{\frac{N}{R} \text{ times}}$, if and only if, subtracting σ^2 from the entries of the diagonal blocks of Σ_g decreases their absolute value. Now, since

the entries of Σ_g are the highest on the diagonal (*i.e.* σ^2), then they start decreasing with the off-diagonals. Therefore, subtracting σ^2 from the entries of the diagonal blocks of Σ_g decreases their absolute value, if and only if, they are greater than $\frac{\sigma^2}{2}$. Consequently, we start decreasing the maximum absolute column sum of the matrix $\Sigma_g - \sigma^2 \underbrace{\text{diag}(\mathbf{1}_{R \times R}, \dots, \mathbf{1}_{R \times R})}_{\frac{N}{R} \text{ times}}$ by increasing

R until we reach $\sigma^2 J_0\left(\frac{2\pi(R-1)}{N-1}W\right) = \frac{\sigma^2}{2}$. More formally,

If R_3^* is the greatest divisor of N verifying

$$J_0\left(\frac{2\pi(R_3^* - 1)}{N - 1}W\right) \leq 0.5, \quad (124)$$

then

$$\|\Sigma_G(R_3^*) - \sigma^2 \mathbb{I}(R_3^*)\|_1 \leq \|\Sigma_G(R) - \sigma^2 \mathbb{I}(R)\|_1 \text{ for all } R \text{ divisor of } N. \quad (125)$$

REFERENCES

- [1] K.-K. Wong, A. Shojaeifard, K.-F. Tong, and Y. Zhang, "Fluid antenna systems," *IEEE Trans. Wireless Commun.*, vol. 20, no. 3, pp. 1950–1962, Mar. 2021.
- [2] K. K. Wong, A. Shojaeifard, K.-F. Tong, and Y. Zhang, "Performance limits of fluid antenna systems," *IEEE Commun. Lett.*, vol. 24, no. 11, pp. 2469–2472, Nov. 2020.
- [3] K.-K. Wong and K.-F. Tong, "Fluid antenna multiple access," *IEEE Trans. Wireless Commun.*, pp. 1–1, Dec. 2021.
- [4] Z. Chai, K.-K. Wong, K.-F. Tong, Y. Chen, and Y. Zhang, "Port selection for fluid antenna systems," *IEEE Commun. Lett.*, pp. 1–1, Feb. 2022.
- [5] G. J. Hayes, J.-H. So, A. Qusba, M. D. Dickey, and G. Lazzi, "Flexible liquid metal alloy (EGaIn) microstrip patch antenna," *IEEE Trans. Antennas Propag.*, vol. 60, no. 5, pp. 2151–2156, May 2012.
- [6] A. M. Morishita, C. K. Y. Kitamura, A. T. Ohta, and W. A. Shiroma, "A liquid-metal monopole array with tunable frequency, gain, and beam steering," *IEEE Antennas Wireless Propag. Lett.*, vol. 12, pp. 1388–1391, Oct. 2013.
- [7] A. Dey, R. Guldiken, and G. Mumcu, "Microfluidically reconfigured wideband frequency-tunable liquid-metal monopole antenna," *IEEE Trans. Antennas Propag.*, vol. 64, no. 6, pp. 2572–2576, Jun. 2016.
- [8] C. Borda-Fortuny, K.-F. Tong, A. Al-Armaghany, and K.-K. Wong, "A low-cost fluid switch for frequency-reconfigurable Vivaldi antenna," *IEEE Antennas Wireless Propag. Lett.*, vol. 16, pp. 3151–3154, Nov. 2017.
- [9] A. Singh, I. Goode, and C. E. Saavedra, "A multistate frequency reconfigurable monopole antenna using fluidic channels," *IEEE Antennas Wireless Propag. Lett.*, vol. 18, no. 5, pp. 856–860, May 2019.
- [10] K. N. Paracha, A. D. Butt, A. S. Alghamdi, S. A. Babale, and P. J. Soh, "Liquid metal antennas: Materials, fabrication and applications," *Sensors*, vol. 20, no. 1, Oct. 2020.
- [11] G. Stüber, *Principles of Mobile Communication*, 4th ed. Springer, 2018.
- [12] A. Goldsmith, *Wireless Communications*. Cambridge University Press, 2005.
- [13] D. Zogas and G. Karagiannidis, "Infinite-series representations associated with the bivariate Rician distribution and their applications," *IEEE Trans. Commun.*, vol. 53, no. 11, pp. 1790–1794, Nov. 2005.
- [14] N. C. Beaulieu and K. T. Hemachandra, "Novel representations for the bivariate Rician distribution," *IEEE Trans. Commun.*, vol. 59, no. 11, pp. 2951–2954, Nov. 2011.

- [15] P. S. Bithas, K. Maliatsos, and A. G. Kanatas, "The bivariate double Rayleigh distribution for multichannel time-varying systems," *IEEE Wireless Commun. Lett.*, vol. 5, no. 5, pp. 524–527, Oct. 2016.
- [16] C. Tan and N. Beaulieu, "Infinite series representations of the bivariate Rayleigh and Nakagami- m distributions," *IEEE Trans. Commun.*, vol. 45, no. 10, pp. 1159–1161, Oct. 1997.
- [17] P. Dharmawansa, N. Rajatheva, and C. Tellambura, "New series representation for the trivariate non-central Chi-squared distribution," *IEEE Trans. Commun.*, vol. 57, no. 3, pp. 665–675, Mar. 2009.
- [18] —, "On the trivariate Rician distribution," *IEEE Trans. Commun.*, vol. 56, no. 12, pp. 1993–1997, Dec. 2008.
- [19] Y. Chen and C. Tellambura, "Infinite series representations of the trivariate and quadrivariate Rayleigh distribution and their applications," *IEEE Trans. Commun.*, vol. 53, no. 12, pp. 2092–2101, Dec. 2005.
- [20] K. D. P. Dharmawansa, R. M. A. P. Rajatheva, and C. Tellambura, "Infinite series representations of the trivariate and quadrivariate Nakagami- m distributions," in *IEEE Int. Conf. Commun.*, Aug. 2007, pp. 1114–1118.
- [21] Y. Chen and C. Tellambura, "Distribution functions of selection combiner output in equally correlated Rayleigh, Rician, and Nakagami- m fading channels," *IEEE Trans. Commun.*, vol. 52, no. 11, pp. 1948–1956, Nov. 2004.
- [22] K. T. Hemachandra and N. C. Beaulieu, "Novel representations for the equicorrelated multivariate non-central Chi-square distribution and applications to MIMO systems in correlated Rician fading," *IEEE Trans. Commun.*, vol. 59, no. 9, pp. 2349–2354, Sep. 2011.
- [23] X. Zhang and N. C. Beaulieu, "Performance analysis of generalized selection combining in generalized correlated Nakagami- m fading," *IEEE Trans. Commun.*, vol. 54, no. 11, pp. 2103–2112, Nov. 2006.
- [24] N. C. Beaulieu and K. T. Hemachandra, "Novel simple representations for gaussian class multivariate distributions with generalized correlation," *IEEE Trans. Inf. Theory*, vol. 57, no. 12, pp. 8072–8083, Dec. 2011.
- [25] X. Zhang and N. C. Beaulieu, "Performance analysis of generalized selection combining in generalized correlated Nakagami- m fading," *IEEE Trans. Commun.*, vol. 54, no. 11, pp. 2103–2112, Nov. 2006.
- [26] Q. Zhang and H. Lu, "A general analytical approach to multi-branch selection combining over various spatially correlated fading channels," *IEEE Trans. Commun.*, vol. 50, no. 7, pp. 1066–1073, Jul. 2002.
- [27] —, "A general analytical approach to multi-branch selection combining over various spatially correlated fading channels," *IEEE Trans. Commun.*, vol. 50, no. 7, pp. 1066–1073, Jul. 2002.
- [28] B. Patrick, *Convergence of Probability Measures*. John Wiley & Sons, 1969.
- [29] R. Mallik, "On multivariate Rayleigh and exponential distributions," *IEEE Trans. Inf. Theory*, vol. 49, no. 6, pp. 1499–1515, Jun. 2003.
- [30] A. Lapidoth, *A Foundation in Digital Communication*, 2nd ed. Cambridge University Press, 2017.
- [31] I. M. Gel'fand and N. Y. Vilenkin, *Generalized functions: Applications of harmonic analysis*. Academic press, 1964, vol. 1–5.
- [32] R. M. Gray, *Toeplitz and Circulant Matrices: A Review*. now, 2006.
- [33] G. C. F. V. L. Golub, "Matrix computations," p. 56, 1996.